



Rectangular multiple-relaxation-time lattice Boltzmann method for the Navier-Stokes and nonlinear convection-diffusion equations: General equilibrium and some important issues

Zhenhua Chai (柴振华)^{1,2,3,*}, Xiaolei Yuan (袁晓垒)^{4,†} and Baochang Shi (施保昌)^{1,2,3,‡}

¹*School of Mathematics and Statistics, Huazhong University of Science and Technology, Wuhan 430074, China*

²*Institute of Interdisciplinary Research for Mathematics and Applied Science, Huazhong University of Science and Technology, Wuhan 430074, China*

³*Hubei Key Laboratory of Engineering Modeling and Scientific Computing, Huazhong University of Science and Technology, Wuhan 430074, China*

⁴*College of Mathematics and Information Science, Hebei University, Baoding 071002, China*



(Received 4 June 2022; revised 26 May 2023; accepted 8 June 2023; published 19 July 2023)

In this paper, we develop a general rectangular multiple-relaxation-time lattice Boltzmann (RMRT-LB) method for the Navier-Stokes equations (NSEs) and nonlinear convection-diffusion equation (NCDE) by extending our recent unified framework of the multiple-relaxation-time lattice Boltzmann (MRT-LB) method [Chai and Shi, *Phys. Rev. E* **102**, 023306 (2020)], where an equilibrium distribution function (EDF) [Lu *et al.*, *Philos. Trans. R. Soc. A* **369**, 2311 (2011)] on a rectangular lattice is utilized. The anisotropy of the lattice tensor on a rectangular lattice leads to anisotropy of the third-order moment of the EDF, which is inconsistent with the isotropy of the viscous stress tensor of the NSEs. To eliminate this inconsistency, we extend the relaxation matrix related to the dynamic and bulk viscosities. As a result, the macroscopic NSEs can be recovered from the RMRT-LB method through the direct Taylor expansion method. Whereas the rectangular lattice does not lead to the change of the zero-, first- and second-order moments of the EDF, the unified framework of the MRT-LB method can be directly applied to the NCDE. It should be noted that the RMRT-LB model for NSEs can be derived on the $rDdQq$ (q discrete velocities in d -dimensional space, $d \geq 1$) lattice, including $rD2Q9$, $rD3Q19$, and $rD3Q27$ lattices, while there are no rectangular $D3Q13$ and $D3Q15$ lattices within this framework of the RMRT-LB method. Thanks to the block-lower triangular relaxation matrix introduced in the unified framework, the RMRT-LB versions (if existing) of the previous MRT-LB models can be obtained, including those based on raw (natural) moment, central moment, Hermite moment, and central Hermite moment. It is also found that when the parameter c_s is an adjustable parameter in the standard or rectangular lattice, the present RMRT-LB method becomes a kind of MRT-LB method for the NSEs and NCDE, and the commonly used MRT-LB models on the $DdQq$ lattice are only its special cases. We also perform some numerical simulations, and the results show that the present RMRT-LB method can give accurate results and also have a good numerical stability.

DOI: [10.1103/PhysRevE.108.015304](https://doi.org/10.1103/PhysRevE.108.015304)

I. INTRODUCTION

The lattice Boltzmann (LB) method, as an effective mesoscopic numerical approach based on kinetic theory, has attained increasing attention and also gained great success in the modeling and simulation of complex fluid flows, heat and mass transfer described by the Navier-Stokes equations (NSEs), and nonlinear convection-diffusion equations (NCDEs) [1–4]. Although many different LB models have been developed in the past three decades, most of them can be viewed as special forms of the multiple-relaxation-time lattice Boltzmann (MRT-LB) model [5], except those with nonlinear collision operators (e.g., the cumulant LB model [6]). The MRT-LB model uses a linear collision operator, i.e., a collision matrix with multiple relaxation parameters,

which extends the commonly used single-relaxation-time LB (SRT-LB) model or lattice Bhatnagar-Gross-Krook (LBGK) model so that the numerical stability and accuracy can be improved by adjusting the free relaxation parameters. Actually, some previous works have shown that the MRT-LB model is superior to the SRT-LB model in terms of accuracy and stability, but only slightly inferior to the SRT-LB model in computational efficiency [5,7,8]. As we know, in the standard LB method for fluid flows, the evolution process is carried out in a highly symmetric lattice space through two steps: collision and propagation. This makes the computational grid and lattice space coupled, resulting in that the standard LB model is generally only implemented on a uniform grid, e.g., the square lattice in two-dimensional space and the cubic lattice in three-dimensional space. It should be noted that this restriction is caused by the requirement on the isotropy of the commonly used standard discrete velocity set, and also limits the applications of the standard LB models. In fact, the nonuniform lattice structure may be more desirable for the problems commonly observed in many fields of science

*hustczh@hust.edu.cn

†yuan_xiaolei2009@163.com

‡Corresponding author: shibc@hust.edu.cn

and engineering, for example, fluid flows with different scales in different coordinate directions, and anisotropic diffusion in porous media.

Historically, there are mainly four ways to design the LB method on a nonuniform grid:

(1) The method in which the computational grid and lattice space are decoupled [9,10] combines the LB approach with some other numerical schemes (e.g., the finite volume scheme, finite difference scheme, and finite element scheme) for the discrete velocity Boltzmann equation (DVBE), and thus both the nonuniform and uniform (isotropic) lattices can be used.

(2) The interpolation-supplemented LB method [11,12] uses the spatial and temporal interpolation schemes to map the information on an inherent grid to a computational grid where the hydrodynamic variables are obtained. Such implementations preserve the main advantages of the standard LB method, and are more flexible in selecting the computational grid. However, to retain the second-order accuracy of the LB method, a second- or higher-order interpolation must be used, which results in additional computational cost. In addition, some undesirable errors and numerical dissipation may be introduced by the interpolation, which in turn brings numerical stability concern.

(3) The LB method with local grid refinement [13–15] divides the whole computational domain into several subdomains, and the standard LB model is used in each subdomain which has its own uniform lattice. Two adjacent subdomains with different lattices may share a common ghost boundary, and the distribution functions (DFs) and/or physical quantities on the ghost boundary need to be determined by some suitable interpolation schemes from both sides of the ghost boundary. Generally, the domain-decomposition technique can be utilized in dividing the domain, and each subdomain can use its own coordinate system and regular lattice [14]. However, the shortcomings caused by interpolation also remain in this method.

(4) The LB method on the rectangular lattice, unlike the above methods, is expected to be a natural and direct extension of the standard LB method on a uniform lattice, and also keeps the *collision-propagation* characteristics of the latter. For NCDE, the anisotropy of the lattice tensor in the LB method on a rectangular lattice does not influence the derivation process of the macroscopic NCDE since the third-order moment of the equilibrium distribution function (EDF) does not appear in the asymptotic analysis [16], and some more discussion on the LB models for NCDEs can be found in previous works [17–21]. Compared to the rectangular LB (RLB) model for NCDE, there is an inconsistency between the anisotropy of the lattice tensor caused by the rectangular lattice and the isotropy of the viscous stress tensor in the NSEs, which brings more difficulties in the development of the RLB models for NSEs. The key to solve the problem is to preserve the isotropy of the lattice tensor or to eliminate the inconsistency caused by the anisotropy of the rectangular lattice tensor. On the one hand, we can improve the isotropy of the lattice tensor by introducing more discrete velocities, while it will bring more computational cost. On the other hand, we can adopt the MRT-LB model such that the inconsistency mentioned above can be eliminated by adjusting the relaxation factors. In fact, when

the SRT collision operator is used, the degrees of freedom of the standard D2Q9 lattice and D3Q19 lattice, and even the D3Q27 lattice, are not enough to remove the anisotropy [22]. As far as we know, Koelman [23] first proposed a SRT-LB model on a rectangular lattice where a low-Mach-number expansion of the Maxwell-Boltzmann distribution is used to obtain the equilibrium distribution function. However, this model fails to recover the correct NSEs with isotropic viscosity when the grid aspect ratio is different from 1. Then, to derive the correct NSEs, several modified rectangular SRT-LB models were proposed. For example, Hegeler *et al.* [22] developed a rectangular SRT-LB model that can derive the correct macroscopic equations by adding discrete velocity directions to increase degrees of freedom. Peng *et al.* [24] and Saadat *et al.* [25] respectively proposed another SRT-LB model on a rectangular grid that can reproduce the correct NSEs by introducing an extended equilibrium distribution function. Besides, Wang and Zhang [26] constructed a SRT-LB model through including some artificial counteracting forcing terms, which are used to remove the anisotropy caused by the rectangular lattice. We note that these SRT-LB models mentioned above can be regarded as some modifications to the standard SRT-LB model by introducing additional discrete velocities, extended equilibrium distribution functions, or force terms, which may bring more computational cost.

Consider the fact that, compared to the SRT-LB model, the MRT-LB model can provide additional degrees of freedom, which can be used to remove this inconsistency between the anisotropy of lattice tensor and the isotropy of viscous stress tensor. Under the framework of the MRT-LB method, Bouzidi *et al.* [27] constructed the first MRT-LB model on a two-dimensional rectangular grid. Although this model can obtain satisfactory results in some numerical tests, the anisotropy problem cannot be overcome completely when the grid aspect ratio is not equal to one [28]. A similar attempt has been made by Zhou [29]; however, this MRT model on the rectangular lattice cannot correctly recover the NSEs. Through an inverse design analysis based on the Chapman-Enskog expansion, Zong *et al.* [28] proposed another MRT-LB model on the D2Q9 rectangular grid, in which an additional adjustable parameter that governs the relative orientation in the energy-normal stress subspace is introduced. By adjusting this parameter, their model can correctly recover the macroscopic equations. However, this model is complicated, and it is difficult to extend it to other lattice structures. After that, Peng *et al.* [30] designed an alternative MRT-LB model on a rectangular grid by incorporating stress components into the equilibrium moments to remove the anisotropy in the viscous stress tensor. Based on the work of Peng *et al.* [30], Wang *et al.* [31] developed a D3Q19 MRT-LB model on a general cuboid grid. However, these two models require a relatively complex quasiequilibrium collision step. In addition, Yahia *et al.* [32] developed a rectangular central-moment MRT-LB model based on a nonorthogonal moment basis, and then extended it to three-dimensional central-moment LB model on a cuboid lattice [33]. The equilibrium to which the central moments relax under collision in this approach is obtained from those corresponding to the continuous Maxwell distribution. These two models involve a relatively complicated computation of the equilibrium moments.

Although the correct macroscopic equations can be derived by introducing artificial source terms [26], additional adjustable parameter [28], or extended equilibrium distribution function [24,25], these treatments are not necessary. Actually, the correct NSEs can be obtained by exploiting the properties of the rectangular MRT-LB (RMRT-LB) model without adding any additional terms. Based on this idea, Zecevic *et al.* [34] presented a RLB method on two- and three-dimensional lattices. They adopted a different set of basis vectors that allows hydrodynamic behavior to be restored through adjusting relaxation parameters. We note that the RMRT-LB model of Zecevic *et al.* [34] still has some certain limitations. For instance, as stated in Ref. [34], there is no orthogonal transformation matrix for the rD3Q19 lattice; thus the RMRT-LB model with rD3Q19 lattice cannot be given [34]. However, the RMRT-LB model with rD3Q19 lattice actually exists. In addition, the equilibrium distribution function and the bulk viscosity in the NSEs are also not considered in Ref. [34].

In this work, we intend to construct a general RMRT-LB method for the Navier-Stokes and nonlinear convection-diffusion equations by extending the recent unified framework of the standard MRT-LB method [16], and derive a general rectangular equilibrium distribution function proposed by Lu *et al.* [35] in detail. Here we would like to point out that in most of the RMRT-LB models, the collision process is carried out in the moment space rather than the velocity (distribution function) space; thus the analysis method (e.g., the Chapman-Enskog expansion) is very complicated and often depends on the specified lattice structure or discrete velocity set. Considering these problems, we will construct a unified framework for the modeling and analysis of the RMRT-LB method in the velocity space, following the previous work [16]. This modeling and analysis approach maintains the simplicity, generality, and efficiency similar to that for the SRT-LB model. For simplicity, we only give some basic elements in the implementation of the RMRT-LB method, including the velocity moments, the weight coefficients of different lattice models (e.g., rD2Q9, rD3Q19, and rD3Q27 lattices), the equilibrium, and auxiliary and source distribution functions. Through the direct Taylor expansion method, the NSEs can be correctly recovered through properly selecting the relaxation submatrix \mathbf{S}_2 , which is related to kinetic and bulk viscosities. In addition, the present RMRT-LB model would reduce to the unified framework of the MRT-LB method [16] with the grid aspect ratio being 1 and sound speed $c_s^2 = c^2/3$. However, if $c_s^2 \neq c^2/3$ and the standard lattice is used, the present RMRT-LB method can be considered as a kind of MRT-LB method for the NSEs and convection-diffusion equations (CDEs) [17,36–38]. We would also like to point out that the present RMRT-LB method is a natural extension to the previous work [16], and it does not introduce any assumptions or additional computational steps. What is more, compared to the available RLB models, the present one is very simple and easy to implement.

The rest of this paper is organized as follows. In Sec. II, the rectangular multiple-relaxation-time lattice Boltzmann method is presented, and the direct Taylor expansion analysis of the present RMRT-LB method is conducted to recover the macroscopic equations in Sec. III. After that, we present the structure of the collision matrix and some special cases of the

RMRT-LB method in Sec. IV. Finally, some conclusions are summarized in Sec. V.

II. RECTANGULAR MULTIPLE-RELAXATION-TIME LATTICE BOLTZMANN METHOD

The evolution equation of the RMRT-LB method with the rectangular $DdQq$ ($rDdQq$) lattice has the same form as that of the MRT-LB method [16]:

$$\begin{aligned} f_j(\mathbf{x} + \mathbf{c}_j \Delta t, t + \Delta t) &= f_j(\mathbf{x}, t) - \Lambda_{jk} f_k^{ne}(\mathbf{x}, t) \\ &+ \Delta t \left[G_j(\mathbf{x}, t) + F_j(\mathbf{x}, t) + \frac{\Delta t}{2} \bar{D}_j F_j(\mathbf{x}, t) \right], \end{aligned} \quad (1)$$

where $f_j(\mathbf{x}, t)$ is the distribution function at position \mathbf{x} in d -dimensional space and time t along the velocity \mathbf{c}_j , $f_j^{ne}(\mathbf{x}, t) = f_j(\mathbf{x}, t) - f_j^{eq}(\mathbf{x}, t)$ is the nonequilibrium distribution function (NEDF), and $f_j^{eq}(\mathbf{x}, t)$ is the EDF. $F_j(\mathbf{x}, t)$ is the distribution function of a source or forcing term, $G_j(\mathbf{x}, t)$ is the auxiliary distribution function, and $\Lambda = (\Lambda_{jk})$ is a $q \times q$ invertible collision matrix. Δt is the time step, $\bar{D}_j = \partial_t + \gamma \mathbf{c}_j \cdot \nabla$ with $\gamma = 1$ for NSEs and $\gamma \in \{0, 1\}$ for the NCDE. In the evolution equation (1), the key elements, \mathbf{c}_j , f_j^{eq} , F_j , G_j and Λ , must be given properly.

The unknown macroscopic conserved variable(s), $\phi(\mathbf{x}, t)$ for the NCDE, or $\rho(\mathbf{x}, t)$ and $\mathbf{u}(\mathbf{x}, t)$ for NSEs, can be computed by

$$\phi(\mathbf{x}, t) = \sum_j f_j(\mathbf{x}, t), \quad (2a)$$

$$\rho(\mathbf{x}, t) = \sum_j f_j(\mathbf{x}, t),$$

$$\mathbf{u}(\mathbf{x}, t) = \sum_j \mathbf{c}_j f_j(\mathbf{x}, t) / \rho(\mathbf{x}, t). \quad (2b)$$

The evolution equation (1) can be divided into two substeps, i.e., collision,

$$\begin{aligned} \tilde{f}_j(\mathbf{x}, t) &= f_j(\mathbf{x}, t) - \Lambda_{jk} f_k^{ne}(\mathbf{x}, t) \\ &+ \Delta t \left[G_j(\mathbf{x}, t) + F_j(\mathbf{x}, t) + \frac{\Delta t}{2} \bar{D}_j F_j(\mathbf{x}, t) \right], \end{aligned} \quad (3a)$$

and propagation,

$$f_j(\mathbf{x} + \mathbf{c}_j \Delta t, t + \Delta t) = \tilde{f}_j(\mathbf{x}, t), \quad (3b)$$

where $\tilde{f}_j(\mathbf{x}, t)$ is the postcollision distribution function.

As pointed out in Ref. [16], in almost all of the MRT-LB models, the collision process in Eq. (1) is carried out in the moment space, and the analysis method (e.g., the popular Chapman-Enskog analysis) is usually more complicated and often depends on the specified lattice structure or discrete velocity set [3,37,39–41]. In this work, we will extend the unified framework of the MRT-LB method [16] to that of the RMRT-LB method.

In the implementation of the RMRT-LB method, there are two popular schemes that can be used to discretize the term $\bar{D}_j F_j(\mathbf{x}, t)$ on the right-hand side of Eq. (1). Actually, if $\gamma = 0$, the first-order explicit difference scheme $\partial_t F_j(\mathbf{x}, t) = [F_j(\mathbf{x}, t) - F_j(\mathbf{x}, t - \Delta t)] / \Delta t$ is adopted for NCDEs [39,42].

For the case of $\gamma = 1$, however, we can use the first-order implicit difference scheme $(\partial_t + \mathbf{c}_j \cdot \nabla)F_j(\mathbf{x}, t) = [F_j(\mathbf{x} + \mathbf{c}_j \Delta t, t + \Delta t) - F_j(\mathbf{x}, t)]/\Delta t$ for both NCDE and NSEs, and take the transform $\tilde{f}_j = f_j - \frac{\Delta t}{2}F_j$ as in Refs. [39,43,44]; then Eq. (1) becomes

$$\begin{aligned} \tilde{f}_j(\mathbf{x} + \mathbf{c}_j \Delta t, t + \Delta t) \\ = \tilde{f}_j(\mathbf{x}, t) - \Lambda_{jk} \tilde{f}_k^{ne}(\mathbf{x}, t) \\ + \Delta t [G_j(\mathbf{x}, t) + (\delta_{jk} - \Lambda_{jk}/2)F_k(\mathbf{x}, t)], \end{aligned} \quad (4)$$

where $\tilde{f}_j^{ne}(\mathbf{x}, t) = \tilde{f}_j(\mathbf{x}, t) - f_j^{eq}(\mathbf{x}, t)$. Additionally, we also have the following relations [36,45,46]:

$$\sum_j f_j(\mathbf{x}, t) = \sum_j \tilde{f}_j(\mathbf{x}, t) + \frac{\Delta t}{2} \sum_j F_j(\mathbf{x}, t), \quad (5a)$$

$$\sum_j \mathbf{c}_j f_j(\mathbf{x}, t) = \sum_j \mathbf{c}_j \tilde{f}_j(\mathbf{x}, t) + \frac{\Delta t}{2} \sum_j \mathbf{c}_j F_j(\mathbf{x}, t). \quad (5b)$$

It follows from Eqs. (2) and (5) that for the NCDE,

$$\phi(\mathbf{x}, t) = \sum_j \tilde{f}_j(\mathbf{x}, t) + \frac{\Delta t}{2} \sum_j F_j(\mathbf{x}, t), \quad (6)$$

or for NSEs,

$$\rho(\mathbf{x}, t) = \sum_j \tilde{f}_j(\mathbf{x}, t) + \frac{\Delta t}{2} \sum_j F_j(\mathbf{x}, t), \quad (7a)$$

$$\mathbf{u}(\mathbf{x}, t) = \left[\sum_j \mathbf{c}_j \tilde{f}_j(\mathbf{x}, t) + \frac{\Delta t}{2} \sum_j \mathbf{c}_j F_j(\mathbf{x}, t) \right] / \rho(\mathbf{x}, t). \quad (7b)$$

III. THE ANALYSIS OF THE RMRT-LB METHOD: DIRECT TAYLOR EXPANSION

There are four basic analysis methods that can be used to recover the macroscopic NSEs and NCDE from the LB models, i.e., the Chapman-Enskog (CE) analysis [21,47,48], the Maxwell iteration (MI) method [49,50], the direct Taylor expansion (DTE) method [51–53], and the recurrence equation (RE) method [20,54,55]. In Ref. [16], these four methods have been compared, and it is shown that they can give the same equations at the second order of expansion parameters, while the DTE method is much simpler. In what follows, only the DTE method is used to analyze the RMRT-LB model for NSEs; a similar analysis for the NCDE can be found in Appendix B.

Applying the Taylor expansion to Eq. (1), one can get

$$\sum_{l=1}^N \frac{\Delta t^l}{l!} D_j^l f_j + O(\Delta t^{N+1}) = -\Lambda_{jk} f_k^{ne} + \Delta t \tilde{F}_j, \quad N \geq 1, \quad (8)$$

where $\tilde{F}_j = G_j + F_j + \Delta t \bar{D}_j F_j / 2$, $D_j = \partial_t + \mathbf{c}_j \cdot \nabla$.

Based on $f_j = f_j^{eq} + f_j^{ne}$ and Eq. (8), the following equations can be obtained:

$$f_j^{ne} = O(\Delta t), \quad (9a)$$

$$\begin{aligned} \sum_{l=1}^{N-1} \frac{\Delta t^l}{l!} D_j^l (f_j^{eq} + f_j^{ne}) + \frac{\Delta t^N}{N!} D_j^N f_j^{eq} \\ = -\Lambda_{jk} f_k^{ne} + \Delta t \tilde{F}_j + O(\Delta t^{N+1}), \quad N \geq 1. \end{aligned} \quad (9b)$$

Then from Eq. (9b), we can derive the equations at first and second orders of Δt ,

$$D_j f_j^{eq} = -\frac{\Lambda_{jk}}{\Delta t} f_k^{ne} + G_j + F_j + O(\Delta t), \quad (10a)$$

$$\begin{aligned} D_j (f_j^{eq} + f_j^{ne}) + \frac{\Delta t}{2} D_j^2 f_j^{eq} = -\frac{\Lambda_{jk}}{\Delta t} f_k^{ne} + G_j + F_j \\ + \frac{\Delta t}{2} \bar{D}_j F_j + O(\Delta t^2). \end{aligned} \quad (10b)$$

According to Eq. (10a), we have

$$\frac{\Delta t}{2} D_j^2 f_j^{eq} = -\frac{1}{2} D_j \Lambda_{jk} f_k^{ne} + \frac{\Delta t}{2} D_j (G_j + F_j) + O(\Delta t^2). \quad (11)$$

Substituting Eq. (11) into Eq. (10b), one can obtain the following equation:

$$\begin{aligned} D_j f_j^{eq} + D_j \left(\delta_{jk} - \frac{\Lambda_{jk}}{2} \right) f_k^{ne} + \frac{\Delta t}{2} D_j G_j \\ = -\frac{\Lambda_{jk}}{\Delta t} f_k^{ne} + G_j + F_j + \frac{\Delta t}{2} (\bar{D}_j - D_j) F_j + O(\Delta t^2). \end{aligned} \quad (12)$$

Based on Eqs. (10a) and (12), the related macroscopic equation (NSEs and NCDE) can be recovered with some proper constraints on the collision matrix Λ and the moments of f_j^{eq} , G_j , and F_j . For NSEs, if we take $\gamma = 1$, then Eq. (12) can be simplified by

$$\begin{aligned} D_j f_j^{eq} + D_j \left(\delta_{jk} - \frac{\Lambda_{jk}}{2} \right) f_k^{ne} + \frac{\Delta t}{2} D_j G_j \\ = -\frac{\Lambda_{jk}}{\Delta t} f_k^{ne} + G_j + F_j + O(\Delta t^2). \end{aligned} \quad (13)$$

For the sake of convenience, we introduce the following matrices:

$$\mathbf{e} = (1, 1, \dots, 1) = (\mathbf{e}_k)_{1 \times q}, \quad (14a)$$

$$\mathbf{E} = (\mathbf{c}_0, \mathbf{c}_1, \dots, \mathbf{c}_{q-1}) = (\mathbf{c}_k)_{d \times q}, \quad (14b)$$

$$\langle \mathbf{E} \mathbf{E} \rangle = (\mathbf{c}_0 \mathbf{c}_0, \mathbf{c}_1 \mathbf{c}_1, \dots, \mathbf{c}_{q-1} \mathbf{c}_{q-1}) = (\mathbf{c}_k \mathbf{c}_k)_{d^2 \times q}, \quad (14c)$$

where \mathbf{e}_k , \mathbf{c}_k , and $\mathbf{c}_k \mathbf{c}_k$ are the k th column of \mathbf{e} , \mathbf{E} , and $\langle \mathbf{E} \mathbf{E} \rangle$, respectively.

A. The derivation of Navier-Stokes equations using DTE method

As pointed out in Ref. [16], the third-order moment of the EDF for the NCDE does not appear in the direct Taylor expansion; therefore, the anisotropy of the lattice tensor on a rectangular lattice would not affect the relevant derivation process for the NCDE. For this reason, we will focus on the RMRT-LB model for NSEs, and the RMRT-LB model for the NCDE is given in Appendix B.

We now consider the following d -dimensional NSEs with the source and forcing terms,

$$\partial_t \rho + \nabla \cdot (\rho \mathbf{u}) = \bar{S}, \quad (15a)$$

$$\partial_t (\rho \mathbf{u}) + \nabla \cdot (\rho \mathbf{u} \mathbf{u}) = -\nabla p + \nabla \cdot \sigma + \bar{\mathbf{F}}, \quad (15b)$$

where the viscous shear stress σ is defined by

$$\begin{aligned}\sigma &= \mu[\nabla\mathbf{u} + (\nabla\mathbf{u})^T] + \lambda(\nabla \cdot \mathbf{u})\mathbf{I} \\ &= \mu\left[\nabla\mathbf{u} + (\nabla\mathbf{u})^T - \frac{2}{d}(\nabla \cdot \mathbf{u})\mathbf{I}\right] + \mu_b(\nabla \cdot \mathbf{u})\mathbf{I},\end{aligned}\quad (16)$$

where μ is the dynamic viscosity, and $\lambda = \mu_b - 2\mu/d$ with μ_b being the bulk viscosity [56,57].

To recover NSEs from the MRT-LB method [Eq. (1)], we need to put some constraints on \mathbf{A} , f_j , f_j^{eq} , G_j , and F_j . In addition, compared to the NCDE [see Eq. (B2) in Appendix B], there is another requirement on the high-order moments of the distribution function for NSEs. Here the following conditions should be satisfied:

$$\begin{aligned}\rho &= \sum_j f_j = \sum_j f_j^{eq}, \\ \rho\mathbf{u} &= \sum_j \mathbf{c}_j f_j = \sum_j \mathbf{c}_j f_j^{eq},\end{aligned}\quad (17a)$$

$$\begin{aligned}\sum_j \mathbf{c}_j \mathbf{c}_j f_j^{eq} &= c_s^2 \rho \mathbf{I} + \rho \mathbf{u} \mathbf{u}, \\ \sum_j \mathbf{c}_j \mathbf{c}_j \mathbf{c}_j f_j^{eq} &= \rho(c_s^2 \mathbf{\Delta} + \bar{\delta}^{(4)}) \cdot \mathbf{u},\end{aligned}\quad (17b)$$

$$\sum_j F_j = \bar{S}, \quad \sum_j \mathbf{c}_j F_j = \bar{\mathbf{F}}, \quad \sum_j \mathbf{c}_j \mathbf{c}_j F_j = \mathbf{0},\quad (17c)$$

$$\begin{aligned}\sum_j G_j &= 0, \quad \sum_j \mathbf{c}_j G_j = \mathbf{0}, \\ \sum_j \mathbf{c}_j \mathbf{c}_j G_j &= \mathbf{M}_{2G},\end{aligned}\quad (17d)$$

$$\begin{aligned}\sum_j \mathbf{e}_j \mathbf{\Lambda}_{jk} &= s_0 \mathbf{e}_k, \quad \sum_j \mathbf{c}_j \mathbf{\Lambda}_{jk} = \mathbf{S}_{10} \mathbf{e}_k + \mathbf{S}_1 \mathbf{c}_k, \\ \sum_j \mathbf{c}_j \mathbf{c}_j \mathbf{\Lambda}_{jk} &= \mathbf{S}_{20} \mathbf{e}_k + \mathbf{S}_{21} \mathbf{c}_k + \mathbf{S}_2 \mathbf{c}_k \mathbf{c}_k,\end{aligned}\quad (17e)$$

where c_s is an adjustable lattice sound speed, $\Delta_{\alpha\beta\gamma\theta} = \delta_{\alpha\beta}\delta_{\gamma\theta} + \delta_{\alpha\gamma}\delta_{\beta\theta} + \delta_{\beta\gamma}\delta_{\alpha\theta}$, and $\bar{\delta}^{(4)}$ is caused by the

anisotropy of the lattice tensor, and is given by

$$\bar{\delta}_{\alpha\beta\gamma\theta}^{(4)} = c_s^2 - 3c_s^2, \quad \alpha = \beta = \gamma = \theta, \quad \bar{\delta}_{\alpha\beta\gamma\theta}^{(4)} = 0, \quad \text{else.}\quad (18)$$

$c_\alpha = \Delta x_\alpha / \Delta t$ ($\alpha = 1, 2, \dots, d$) in d -dimensional space with Δx_α being the spacing step in the α axis. \mathbf{M}_{2G} is a second-order tensor to be determined below, \mathbf{S}_{10} is a $d \times 1$ matrix, \mathbf{S}_1 is an invertible $d \times d$ relaxation submatrix, \mathbf{S}_{20} and \mathbf{S}_{21} are two $d^2 \times 1$ and $d^2 \times d$ matrices, and \mathbf{S}_2 is an invertible $d^2 \times d^2$ relaxation submatrix corresponding to the dynamic and bulk viscosities. Additionally, Eq. (17a) gives the following conditions:

$$\begin{aligned}\sum_j f_j^{ne} &= \sum_j (f_j - f_j^{eq}) = 0, \\ \sum_j \mathbf{c}_j f_j^{ne} &= \sum_j \mathbf{c}_j (f_j - f_j^{eq}) = \mathbf{0},\end{aligned}\quad (19)$$

which are the mass and momentum conservation.

Summing Eq. (13) and adopting Eqs. (17) and (19), one can obtain

$$\partial_t \rho + \nabla \cdot (\rho \mathbf{u}) = \bar{S} + O(\Delta t^2),\quad (20)$$

which indicates that the continuity equation (15a) is recovered correctly at $O(\Delta t^2)$.

Multiplying \mathbf{c}_j on both sides of Eqs. (10a) and (13), and through a summation over j , we have

$$\partial_t (\rho \mathbf{u}) + \nabla \cdot (c_s^2 \rho \mathbf{I} + \rho \mathbf{u} \mathbf{u}) = \bar{\mathbf{F}} + O(\Delta t),\quad (21a)$$

$$\begin{aligned}\partial_t (\rho \mathbf{u}) + \nabla \cdot (c_s^2 \rho \mathbf{I} + \rho \mathbf{u} \mathbf{u}) + \nabla \cdot (\mathbf{I} - \mathbf{S}_2/2) \sum_k \mathbf{c}_k \mathbf{c}_k f_k^{(ne)} \\ + \frac{\Delta t}{2} \nabla \cdot \mathbf{M}_{2G} = \bar{\mathbf{F}} + O(\Delta t^2),\end{aligned}\quad (21b)$$

where Eqs. (17) and (19) have been used. In addition, from Eqs. (10a), (17), and (20) we get

$$\begin{aligned}\sum_k \mathbf{c}_k \mathbf{c}_k f_k^{ne} &= -\Delta t \mathbf{S}_2^{-1} \sum_k \mathbf{c}_k \mathbf{c}_k (D_k f_k^{eq} - G_k - F_k) + O(\Delta t^2) \\ &= -\Delta t \mathbf{S}_2^{-1} \left[\partial_t \sum_k \mathbf{c}_k \mathbf{c}_k f_k^{eq} + \nabla \cdot \sum_k \mathbf{c}_k \mathbf{c}_k \mathbf{c}_k f_k^{eq} - \mathbf{M}_{2G} \right] + O(\Delta t^2) \\ &= -\Delta t \mathbf{S}_2^{-1} \left[\partial_t (c_s^2 \rho \mathbf{I} + \rho \mathbf{u} \mathbf{u}) + \nabla \cdot (\rho(c_s^2 \mathbf{\Delta} + \bar{\delta}^{(4)}) \cdot \mathbf{u}) - \mathbf{M}_{2G} \right] + O(\Delta t^2) \\ &= -\Delta t \mathbf{S}_2^{-1} \left[\partial_t (\rho \mathbf{u} \mathbf{u}) + c_s^2 (\nabla \rho \mathbf{u} + (\nabla \rho \mathbf{u})^T) + \nabla \cdot (\rho \bar{\delta}^{(4)} \cdot \mathbf{u}) + c_s^2 \bar{S} \mathbf{I} - \mathbf{M}_{2G} \right] + O(\Delta t^2).\end{aligned}\quad (22)$$

Based on Eqs. (20) and (21a), the following equations can be obtained:

$$\partial_t (\rho \mathbf{u} \mathbf{u}) = \mathbf{u} \bar{\mathbf{F}} + \bar{\mathbf{F}} \mathbf{u} - c_s^2 [\mathbf{u} \nabla \rho + (\mathbf{u} \nabla \rho)^T] - \nabla \cdot (\rho \mathbf{u} \mathbf{u} \mathbf{u}) - \mathbf{u} \mathbf{u} \bar{S} + O(\Delta t \text{Ma}),\quad (23a)$$

$$c_s^2 [\nabla \rho \mathbf{u} + (\nabla \rho \mathbf{u})^T] = c_s^2 \rho [\nabla \mathbf{u} + (\nabla \mathbf{u})^T] + c_s^2 [\mathbf{u} \nabla \rho + (\mathbf{u} \nabla \rho)^T],\quad (23b)$$

$$\nabla \cdot (\rho \bar{\delta}^{(4)} \cdot \mathbf{u}) = \rho \nabla \cdot (\bar{\delta}^{(4)} \cdot \mathbf{u}) + O(\text{Ma}^3),\quad (23c)$$

then we can rewrite Eq. (22) as

$$\sum_k \mathbf{c}_k \mathbf{c}_k f_k^{ne} = -\Delta t \mathbf{S}_2^{-1} \left[\rho c_s^2 (\nabla \mathbf{u} + (\nabla \mathbf{u})^T) + \rho \nabla \cdot (\bar{\delta}^{(4)} \cdot \mathbf{u}) + \mathbf{u} \bar{\mathbf{F}} + \bar{\mathbf{F}} \mathbf{u} + (c_s^2 \mathbf{I} - \mathbf{u} \mathbf{u}) \bar{S} - \mathbf{M}_{2G} \right] + O(\Delta t^2 + \Delta t \text{Ma}^3),\quad (24)$$

where Ma is the Mach number, and the relations $\nabla\rho = O(Ma^2)$, $\mathbf{u} = O(Ma)$, and $\nabla \cdot (\rho\mathbf{u}\mathbf{u}) = O(Ma^3)$ have been used.

Substituting Eq. (24) into Eq. (21b) and using Eq. (17), we can obtain

$$\begin{aligned} \partial_t(\rho\mathbf{u}) + \nabla \cdot (c_s^2\rho\mathbf{I} + \rho\mathbf{u}\mathbf{u}) &= \Delta t \nabla \cdot [\rho(\mathbf{S}_2^{-1} - \mathbf{I}/2)(c_s^2(\nabla\mathbf{u} + (\nabla\mathbf{u})^T) + \nabla \cdot (\bar{\delta}^{(4)} \cdot \mathbf{u}))] \\ &\quad + \bar{\mathbf{F}} + \Delta t \nabla \cdot \mathbf{R}\mathbf{H}_2 + O(\Delta t^2 + \Delta t Ma^3), \end{aligned} \quad (25)$$

where

$$\mathbf{R}\mathbf{H}_2 = (\mathbf{S}_2^{-1} - \mathbf{I}/2)(\mathbf{u}\bar{\mathbf{F}} + \bar{\mathbf{F}}\mathbf{u} + (c_s^2\mathbf{I} - \mathbf{u}\mathbf{u})\bar{\mathcal{S}}) - \mathbf{S}_2^{-1}\mathbf{M}_{2G}. \quad (26)$$

To obtain the correct NSEs, $\mathbf{R}\mathbf{H}_2 = 0$ should be satisfied, which gives the following equation:

$$\mathbf{M}_{2G} = (\mathbf{I} - \mathbf{S}_2/2)(\mathbf{u}\bar{\mathbf{F}} + \bar{\mathbf{F}}\mathbf{u} + (c_s^2\mathbf{I} - \mathbf{u}\mathbf{u})\bar{\mathcal{S}}). \quad (27)$$

Then Eq. (25) can be rewritten as

$$\partial_t(\rho\mathbf{u}) + \nabla \cdot (c_s^2\rho\mathbf{I} + \rho\mathbf{u}\mathbf{u}) = \nabla \cdot \tau + \bar{\mathbf{F}} + O(\Delta t^2 + \Delta t Ma^3), \quad (28)$$

where

$$\tau = \Delta t \rho (\mathbf{S}_2^{-1} - \mathbf{I}/2) [c_s^2(\nabla\mathbf{u} + (\nabla\mathbf{u})^T) + \nabla \cdot (\bar{\delta}^{(4)} \cdot \mathbf{u})], \quad (29)$$

which needs to be determined as a viscous term through selecting the proper relaxation matrix \mathbf{S}_2^{-1} .

Let

$$\mathbf{S}_2^{-1} = \begin{pmatrix} \mathbf{S}_2^{(1)} & 0 \\ 0 & \mathbf{S}_2^{(2)} \end{pmatrix}, \quad (30)$$

with

$$\mathbf{S}_2^{(1)} = \text{diag}(s_{\alpha\alpha}^{-1}) + \mathbf{a}\mathbf{b}^T/d, \quad \mathbf{S}_2^{(2)} = \text{diag}(s_{\alpha\beta}^{-1})_{\alpha \neq \beta}, \quad (31)$$

where $\mathbf{a} = (a_\alpha)$, $\mathbf{b} = (b_\beta)$ with $a_\alpha = (s_{b\alpha}^{-1} - s_{\alpha\alpha}^{-1})(c_\alpha^2 - c_s^2)$ and $b_\beta = 1/(c_\beta^2 - c_s^2)$. Then substituting Eq. (30) into Eq. (29), one can obtain the viscous shear stress,

$$\tau = \mu \left[\nabla\mathbf{u} + (\nabla\mathbf{u})^T - \frac{2}{d}(\nabla \cdot \mathbf{u})\mathbf{I} \right] + \mu_b [(\nabla \cdot \mathbf{u})\mathbf{I}], \quad (32)$$

where μ and μ_b are dynamic and bulk viscosities,

$$\begin{aligned} \mu &= \left(s_{\alpha\beta}^{-1} - \frac{1}{2} \right) \rho c_s^2 \Delta t, \quad \alpha \neq \beta, \\ \mu &= \frac{1}{2} \left(s_{\alpha\alpha}^{-1} - \frac{1}{2} \right) \rho (c_\alpha^2 - c_s^2) \Delta t, \end{aligned} \quad (33a)$$

$$\mu_b = \frac{1}{d} \left(s_{b\alpha}^{-1} - \frac{1}{2} \right) \rho (c_\alpha^2 - c_s^2) \Delta t. \quad (33b)$$

When $p = \rho c_s^2$ and the truncation error $O(\Delta t^2 + \Delta t Ma^3)$ is neglected, Eq. (28) becomes

$$\begin{aligned} \partial_t(\rho\mathbf{u}) + \nabla \cdot (p\mathbf{I} + \rho\mathbf{u}\mathbf{u}) &= \nabla \cdot \mu \left[\nabla\mathbf{u} + (\nabla\mathbf{u})^T - \frac{2}{d}(\nabla \cdot \mathbf{u})\mathbf{I} \right] \\ &\quad + \nabla \cdot \mu_b [(\nabla \cdot \mathbf{u})\mathbf{I}] + \bar{\mathbf{F}}, \end{aligned} \quad (34)$$

which are NSEs (15) with dynamic and bulk viscosities defined by Eq. (33).

From Eq. (33a) one can find that there is no any SRT version of the RMRT-LB model since at least two different relaxation parameters are needed for the rDdQq lattice with different c_α .

Remark 1. We note that one can obtain the following generalized viscous shear stress from Eq. (29),

$$\tau = \mathbf{K}_\mu \left[\nabla\mathbf{u} + (\nabla\mathbf{u})^T - \frac{2}{d}(\nabla \cdot \mathbf{u})\mathbf{I} \right] + \mathbf{K}_{\mu_b} [(\nabla \cdot \mathbf{u})\mathbf{I}], \quad (35)$$

with \mathbf{K}_μ and \mathbf{K}_{μ_b} being dynamic and bulk viscosity tensors,

$$\begin{aligned} \mathbf{K}_{\mu,\alpha\beta} &= \left(s_{\alpha\beta}^{-1} - \frac{1}{2} \right) \rho c_s^2 \Delta t, \quad \alpha \neq \beta, \\ \mathbf{K}_{\mu,\alpha\alpha} &= \frac{1}{2} \left(s_{\alpha\alpha}^{-1} - \frac{1}{2} \right) \rho (c_\alpha^2 - c_s^2) \Delta t, \end{aligned} \quad (36a)$$

$$\mathbf{K}_{\mu_b,\alpha\alpha} = \frac{1}{d} \left(s_{b\alpha}^{-1} - \frac{1}{2} \right) \rho (c_\alpha^2 - c_s^2) \Delta t. \quad (36b)$$

Then the following generalized NSEs can be obtained:

$$\begin{aligned} \partial_t(\rho\mathbf{u}) + \nabla \cdot (p\mathbf{I} + \rho\mathbf{u}\mathbf{u}) &= \nabla \cdot \mathbf{K}_\mu \left[\nabla\mathbf{u} + (\nabla\mathbf{u})^T - \frac{2}{d}(\nabla \cdot \mathbf{u})\mathbf{I} \right] \\ &\quad + \nabla \cdot [\mathbf{K}_{\mu_b} [(\nabla \cdot \mathbf{u})\mathbf{I}] + \bar{\mathbf{F}}]. \end{aligned} \quad (37)$$

The physical meaning and applications of this equation need to be considered in the future.

It should be noted that, due to its inherent characteristics, the present RMRT-LB model can correctly recover the NSEs [Eq. (15)], while it is only suitable for incompressible or weakly compressible fluid flows since the third-order term in the Mach number has been omitted, as discussed above. Finally, we also present a local scheme to calculate the viscous shear stress or strain rate tensor in the framework of the LB method [40,58,59]. From Eqs. (24), (32), and (33), one can obtain different approximate formulas for the viscous shear stress,

$$\begin{aligned} \tau &= -(\mathbf{I} - \mathbf{S}_2/2) \left[\sum_k \mathbf{c}_k \mathbf{c}_k f_k^{ne} + \frac{\Delta t}{2} (\mathbf{u}\bar{\mathbf{F}} + \bar{\mathbf{F}}\mathbf{u} + (c_s^2\mathbf{I} - \mathbf{u}\mathbf{u})\bar{\mathcal{S}}) \right] + O(\Delta t^2 + \Delta t Ma^3) \\ &= -(\mathbf{I} - \mathbf{S}_2/2) \left[\sum_k \mathbf{c}_k \mathbf{c}_k f_k^{ne} + \frac{\Delta t}{2} (\mathbf{u}\bar{\mathbf{F}} + \bar{\mathbf{F}}\mathbf{u} + c_s^2\bar{\mathcal{S}}\mathbf{I}) \right] + O(\Delta t^2 + \Delta t Ma^3) \\ &= -(\mathbf{I} - \mathbf{S}_2/2) \left[\sum_k \mathbf{c}_k \mathbf{c}_k f_k^{ne} + \frac{\Delta t}{2} c_s^2 \bar{\mathcal{S}}\mathbf{I} \right] + O(\Delta t^2 + \Delta t Ma^2), \end{aligned} \quad (38)$$

where $\mathbf{u}\bar{\mathbf{u}} = O(\text{Ma}^3)$ and $\mathbf{u}\bar{\mathbf{F}} + \bar{\mathbf{F}}\mathbf{u} = O(\text{Ma}^2)$ are used.

For incompressible fluid flows, the term $O(\Delta t^2 + \Delta t\text{Ma}^3)$ in Eq. (38) can be neglected; then the following local scheme for viscous stress with a second-order accuracy in time can be obtained from Eq. (38):

$$\mu(\nabla\mathbf{u} + (\nabla\mathbf{u})^T) = -(\mathbf{I} - \mathbf{S}_2/2) \left[\sum_k \mathbf{c}_k \mathbf{c}_k f_k^{ne} + \frac{\Delta t}{2} (\mathbf{u}\bar{\mathbf{F}} + \bar{\mathbf{F}}\mathbf{u} + c_s^2 \bar{\mathbf{S}}\mathbf{I}) \right], \quad (39)$$

where \mathbf{S}_2 is a diagonal matrix with $\mathbf{S}_{2,\alpha\alpha} = s_{s\alpha}$, and $\mathbf{S}_{2,\alpha\beta} = s_{\alpha\beta}$ ($\alpha \neq \beta$).

Based on Eq. (39), one can also give an expression of strain rate tensor with a second-order accuracy in time,

$$\frac{\nabla\mathbf{u} + (\nabla\mathbf{u})^T}{2} = -(\mu^{-1}/2)(\mathbf{I} - \mathbf{S}_2/2) \left[\sum_k \mathbf{c}_k \mathbf{c}_k f_k^{ne} + \frac{\Delta t}{2} (\mathbf{u}\bar{\mathbf{F}} + \bar{\mathbf{F}}\mathbf{u} + c_s^2 \bar{\mathbf{S}}\mathbf{I}) \right]. \quad (40)$$

It should be noted that if the term $\mathbf{u}\bar{\mathbf{F}} + \bar{\mathbf{F}}\mathbf{u}$ in Eqs. (27), (39), and (40) is neglected, the much simpler formulas can be obtained with the truncation error $O(\Delta t^2 + \Delta t\text{Ma}^2)$.

In addition, from Eqs. (38) and (39) we obtain

$$\begin{aligned} \sum_k \mathbf{c}_k \mathbf{c}_k f_k^{ne} &= -(\mathbf{I} - \mathbf{S}_2/2)^{-1} \tau - \frac{\Delta t}{2} (\mathbf{u}\bar{\mathbf{F}} + \bar{\mathbf{F}}\mathbf{u} + c_s^2 \bar{\mathbf{S}}\mathbf{I}) + O(\Delta t^2 + \Delta t\text{Ma}^3) \\ &= -(\mathbf{I} - \mathbf{S}_2/2)^{-1} \tau - \frac{\Delta t}{2} c_s^2 \bar{\mathbf{S}}\mathbf{I} + O(\Delta t^2 + \Delta t\text{Ma}^2), \end{aligned} \quad (41)$$

$$\begin{aligned} \sum_k \mathbf{c}_k \mathbf{c}_k f_k^{ne} &= -(\mathbf{I} - \mathbf{S}_2/2)^{-1} \mu(\nabla\mathbf{u} + (\nabla\mathbf{u})^T) - \frac{\Delta t}{2} (\mathbf{u}\bar{\mathbf{F}} + \bar{\mathbf{F}}\mathbf{u} + c_s^2 \bar{\mathbf{S}}\mathbf{I}) + O(\Delta t^2 + \Delta t\text{Ma}^3) \\ &= -(\mathbf{I} - \mathbf{S}_2/2)^{-1} \mu(\nabla\mathbf{u} + (\nabla\mathbf{u})^T) - \frac{\Delta t}{2} c_s^2 \bar{\mathbf{S}}\mathbf{I} + O(\Delta t^2 + \Delta t\text{Ma}^2). \end{aligned} \quad (42)$$

If we introduce $\mathbf{m}_2^{ne} = \sum_k \mathbf{c}_k \mathbf{c}_k f_k^{ne}$ and utilize Eqs. (19), (41), (42), and (44) with $c_{s\alpha} = c_s$ for all α , one can derive a useful formula to approximate f_j^{ne} ,

$$f_j^{ne} = g_j^{eq}(0, \mathbf{0}, \mathbf{m}_2^{ne}) = \omega_j \tilde{\mathbf{Q}}_j : \mathbf{m}_2^{ne} = \omega_j \left[\sum_{\alpha} \frac{\mathbf{m}_{2,\alpha\alpha}^{ne} (c_{j\alpha}^2 - c_s^2)}{c_s^2 (c_{\alpha}^2 - c_s^2)} + \sum_{\bar{\alpha} \neq \alpha} \frac{\mathbf{m}_{2,\alpha\bar{\alpha}}^{ne} (c_{j\alpha} c_{j\bar{\alpha}})}{2c_s^4} \right], \quad (43)$$

where $\bar{\alpha}$ denotes the index γ with $\gamma \neq \alpha$. Equation (43) is an extension of the formula given by Guo and Zhao in Ref. [10] when $\mathbf{\Lambda} = \mathbf{S} = \mathbf{I}/\tau$ (τ is the relaxation time), $c_{\alpha} = c$, and $c_s^2 = c^2/3$, and it can also be used for the initialization of f_j .

B. The equilibrium, auxiliary, and source distribution functions of the RMRT-LB method for NSEs

From the above analysis, one can clearly observe that to recover the macroscopic NSEs (15) from RMRT-LB method (1), the equilibrium, auxiliary, and source distribution functions should satisfy some necessary requirements, as depicted by Eq. (17). In this work, we would consider the common quadratic form of the EDF. Actually, the EDF is not unique [18,21,38], but it must satisfy some basic moment conditions.

Based on the previous work [35], we first present the following EDF with a general quadratic form on the rDdQq lattice, which can be viewed as an extension of the commonly used one,

$$g_j^{eq}(\mathbf{A}, \mathbf{B}, \mathbf{M}) = \omega_j (\mathbf{A} + \tilde{\mathbf{c}}_j \cdot \mathbf{B} + \tilde{\mathbf{Q}}_j : \mathbf{M}), \quad (44)$$

where ω_j is the weight coefficient (see Appendix A), and

$$\begin{aligned} \tilde{\mathbf{c}}_{j\alpha} &= \mathbf{c}_{j\alpha} / c_{s\alpha}^2, \quad \tilde{\mathbf{Q}}_{j\alpha\alpha} = \mathbf{Q}_{j\alpha\alpha} / (c_{s\alpha}^2 (c_{\alpha}^2 - c_{s\alpha}^2)), \\ \tilde{\mathbf{Q}}_{j\alpha\beta} &= \mathbf{Q}_{j\alpha\beta} / (2c_{s\alpha}^2 c_{s\beta}^2) \quad (\alpha \neq \beta), \quad \mathbf{Q}_j = \mathbf{c}_j \mathbf{c}_j - \mathbf{\Delta}^{(2)}. \end{aligned} \quad (45)$$

Here $\mathbf{\Delta}^{(2)}$ is given by Eq. (A6) in Appendix A. We would also like to point out that, strictly speaking, $c_{s\alpha}$ is direction dependent; while it is usually taken to be a direction-independent form with $c_{s\alpha} = c_s$, c_s is an adjustable parameter [17,36–38,60].

According to the properties of rDdQq lattice models, and after some algebraic manipulations, we can obtain the basic moments of g_j^{eq} on the rDdQq lattice [35],

$$\begin{aligned} \sum_j g_j^{eq} &= A, \quad \sum_j \mathbf{c}_j g_j^{eq} = \mathbf{B}, \\ \sum_j \mathbf{c}_j \mathbf{c}_j g_j^{eq} &= A \mathbf{\Delta}^{(2)} + \mathbf{M}, \end{aligned} \quad (46a)$$

$$\sum_j \mathbf{c}_j \mathbf{c}_j \mathbf{c}_j g_j^{eq} = \mathbf{\Delta}^{(4)} \cdot \tilde{\mathbf{B}}, \quad (46b)$$

where $\tilde{\mathbf{B}}_{\alpha} = \mathbf{B}_{\alpha} / c_{s\alpha}^2$, $\mathbf{\Delta}^{(4)} = \langle \mathbf{\Delta}^{(2)} \mathbf{\Delta}^{(2)} \rangle + \delta^{(4)}$, which is defined by Eq. (A19).

With the help of Eq. (A19), we can rewrite Eq. (46b) as

$$\sum_j \mathbf{c}_{j\alpha} \mathbf{c}_{j\beta} \mathbf{c}_{j\gamma} g_j^{eq} = \Delta_{\alpha\beta}^{(2)} B_{\gamma} + \Delta_{\alpha\gamma}^{(2)} B_{\beta} + \Delta_{\beta\gamma}^{(2)} B_{\alpha} + \delta_{\alpha\beta\gamma\theta}^{(4)} \tilde{B}_{\theta}. \quad (47)$$

For a rDdQq lattice model, to satisfy the moment conditions in Eq. (17), the explicit expressions of f_j^{eq} , G_j , and F_j with $c_{s\alpha} = c_s$ for all α can be given by

$$\begin{aligned} f_j^{eq} &= g_j^{eq}(\rho, \rho \mathbf{u}, \rho \mathbf{u}\mathbf{u}) = \rho g_j^{eq}(1, \mathbf{u}, \mathbf{u}\mathbf{u}) \\ &= \omega_j \rho \left[1 + \frac{\mathbf{c}_{j\alpha} \mathbf{u}_\alpha}{c_s^2} + \frac{u_\alpha^2 (c_{j\alpha}^2 - c_s^2)}{c_s^2 (c_\alpha^2 - c_s^2)} + \frac{u_\alpha u_{\bar{\alpha}} (c_{j\alpha} c_{j\bar{\alpha}})}{2c_s^4} \right], \end{aligned} \quad (48)$$

$$\begin{aligned} G_j &= g_j^{eq}(0, \mathbf{0}, \mathbf{M}_{2G}) \\ &= \omega_j \left[\frac{\mathbf{M}_{2G, \alpha\alpha} (c_{j\alpha}^2 - c_s^2)}{c_s^2 (c_\alpha^2 - c_s^2)} + \frac{\mathbf{M}_{2G, \alpha\bar{\alpha}} (c_{j\alpha} c_{j\bar{\alpha}})}{2c_s^4} \right], \end{aligned} \quad (49)$$

$$F_j = g_j^{eq}(\bar{s}, \bar{\mathbf{F}}, -c_s^2 \bar{s} \mathbf{I}) = \omega_j \left[\bar{s} + \frac{\mathbf{c}_{j\alpha} \bar{\mathbf{F}}_\alpha}{c_s^2} - \bar{s} \frac{e_\alpha (c_{j\alpha}^2 - c_s^2)}{c_\alpha^2 - c_s^2} \right], \quad (50)$$

where \mathbf{M}_{2G} is determined by Eq. (27), and can also be computed by

$$\mathbf{M}_{2G} = (\mathbf{I} - \mathbf{S}_2/2)(\mathbf{u}\bar{\mathbf{F}} + \bar{\mathbf{F}}\mathbf{u} + c_s^2 \bar{s} \mathbf{I}), \quad (51)$$

where $\mathbf{u}\bar{s} = O(\text{Ma}^3)$ has been used to derive Eq. (51).

From the above discussion, one can find that the NSEs and NCDE can be recovered correctly from the RMRT-LB method through the DTE method. In other words, the present RMRT-LB method not only can be used to study fluid flow problems governed by the NSEs, but also can be adopted to investigate the heat and mass transport problems depicted by the coupled NCDE(s) and NSEs.

Remark 2. The second-order moment of f_j^{ne} , i.e., $\langle \mathbf{E}\mathbf{E} \rangle \mathbf{f}^{ne} = \sum_k \mathbf{c}_k \mathbf{c}_k f_k^{ne}$ in Eqs. (39) or (40), can be computed by its counterpart ($\langle \mathbf{E}\mathbf{E} \rangle \mathbf{f}^{ne} = \mathbf{m}^{ne}_{(\mathbf{E}\mathbf{E})} = \mathbf{m}_{(\mathbf{E}\mathbf{E})} - \mathbf{m}_{(\mathbf{E}\mathbf{E})}^{eq}$) in the moment space [see Eqs. (53) or (54)].

Remark 3. It can be seen from Eq. (36) that the RMRT-LB model on a rectangular or standard lattice with $c_s^2 \neq c^2/3$ does not have the versions of the SRT-LB model and two-relaxation-time lattice Boltzmann (TRT-LB) model [38,61]; this is because there are at least two different relaxation factors related to the second-order moment of f_j^{eq} (or to the dynamic viscosity μ). Keeping this in mind, we can find that the RMRT-LB model in Ref. [27] has only one relaxation factor s_μ related to the viscosity μ ; thus it cannot recover NSEs (15) correctly.

Remark 4. For the standard lattice, if $c_s^2 \neq c^2/3$, we can obtain the forms of f_j^{eq} , G_j , and F_j defined by Eqs. (48)–(50) for NSEs, which gives a kind of MRT-LB model with the sound speed c_s as an adjustable parameter.

Remark 5. Inserting $\rho = \rho_0 + \delta\rho$ with $\delta\rho = O(\text{Ma}^2)$ into Eq. (48), and omitting the terms of $O(\text{Ma}^3)$, one can obtain the previous LB model [62] from the present RMRT-LB model with $f_j^{eq} = g_j^{eq}(\rho, \rho_0 \mathbf{u}, \rho_0 \mathbf{u}\mathbf{u})$.

Remark 6. Under the assumption of low Mach number, we can take $\mathbf{a} = 0$ or $s_{b\alpha}^{-1} = s_\alpha^{-1}$ for all α in Eq. (31); thus \mathbf{S}_2^{-1} can be simplified by a diagonal matrix.

IV. STRUCTURE OF COLLISION MATRIX AND SOME SPECIAL CASES OF THE RMRT-LB METHOD

A. Structure of collision matrix

As we know, the MRT-LB model can also be analyzed and implemented in moment space. When the discrete velocity set $V_q = \{\mathbf{c}_j, 0 \leq j \leq q-1\}$ or the rDdQq lattice model is given, we can construct different forms of collision matrix \mathbf{A} in the RMRT-LB method [Eq. (1)]. In general, the commonly used collision matrix \mathbf{A} satisfying the constraints in Eq. (17) or Eq. (B2) has the following form [16]:

$$\mathbf{A} = \mathbf{M}^{-1} \mathbf{S} \mathbf{M}, \quad (52a)$$

$$\mathbf{S} = (\mathbf{S}_{kj}), \quad \mathbf{S}_{kj} = 0 \ (k < j), \quad \mathbf{S}_{kk} = \mathbf{S}_k, \quad (52b)$$

where $\mathbf{M} \in R^{q \times q}$ is an invertible transformation matrix, whose rows are composed of discrete velocities in V_q , \mathbf{S} is a block-lower-triangle matrix, $\mathbf{S}_k \in R^{n_k \times n_k}$ is a relaxation matrix corresponding to the k th-order ($0 \leq k \leq m$) moment of discrete velocity.

Given a transformation matrix \mathbf{M} , let $\mathbf{f} = (f_0, f_1, \dots, f_{q-1})^T$, $\mathbf{f}^{eq} = (f_0^{eq}, f_1^{eq}, \dots, f_{q-1}^{eq})^T$, then one can execute the transformation between velocity space and moment space,

$$\mathbf{m} = \mathbf{M} \mathbf{f}, \quad \mathbf{m}^{eq} = \mathbf{M} \mathbf{f}^{eq}, \quad (53)$$

or equivalently,

$$\mathbf{f} = \mathbf{M}^{-1} \mathbf{m}, \quad \mathbf{f}^{eq} = \mathbf{M}^{-1} \mathbf{m}^{eq}. \quad (54)$$

Using Eqs. (52)–(54), the evolution equation of the RMRT-LB method [Eqs. (3)] can be written in a matrix form, for collision in moment space,

$$\begin{aligned} \tilde{\mathbf{m}}(\mathbf{x}, t) &= \mathbf{m}(\mathbf{x}, t) - \mathbf{S} \mathbf{m}^{ne}(\mathbf{x}, t) \\ &+ \Delta t \left[\mathbf{m}_G(\mathbf{x}, t) + \mathbf{m}_F(\mathbf{x}, t) + \frac{\Delta t}{2} \tilde{\mathbf{D}} \mathbf{m}_F(\mathbf{x}, t) \right], \end{aligned} \quad (55a)$$

and propagation in velocity space,

$$\mathbf{f}(\mathbf{x} + \mathbf{c}_j \Delta t, t + \Delta t) = \mathbf{M}^{-1} \tilde{\mathbf{m}}(\mathbf{x}, t), \quad (55b)$$

where $\mathbf{f}(\mathbf{x} + \mathbf{c}_j \Delta t, t + \Delta t) = (f_0(\mathbf{x} + \mathbf{c}_0 \Delta t, t + \Delta t), f_1(\mathbf{x} + \mathbf{c}_1 \Delta t, t + \Delta t), \dots, f_{q-1}(\mathbf{x} + \mathbf{c}_{q-1} \Delta t, t + \Delta t))^T$, $\mathbf{m}^{ne} = \mathbf{m} - \mathbf{m}^{eq}$, $\mathbf{m}_G = \mathbf{M} \mathbf{G}$, $\mathbf{m}_F = \mathbf{M} \mathbf{F}$, $\mathbf{G} = (G_0, G_1, \dots, G_{q-1})^T$, $\mathbf{F} = (F_0, F_1, \dots, F_{q-1})^T$, and $\tilde{\mathbf{D}} = \mathbf{M}^{-1} \mathbf{diag}(\tilde{D}_j) \mathbf{M}$. On the other hand, one can also implement the RMRT-LB method [Eqs. (3)] in the velocity space, for collision,

$$\begin{aligned} \tilde{\mathbf{f}}(\mathbf{x}, t) &= \mathbf{M}^{-1} (\mathbf{m}(\mathbf{x}, t) - \mathbf{S} \mathbf{m}^{ne}(\mathbf{x}, t)) \\ &+ \Delta t \left[\mathbf{G}(\mathbf{x}, t) + \mathbf{F}(\mathbf{x}, t) + \frac{\Delta t}{2} \mathbf{diag}(\tilde{D}_j) \mathbf{F}(\mathbf{x}, t) \right], \end{aligned} \quad (56a)$$

and propagation,

$$\mathbf{f}(\mathbf{x} + \mathbf{c}_j \Delta t, t + \Delta t) = \tilde{\mathbf{f}}(\mathbf{x}, t). \quad (56b)$$

Similarly, the RMRT-LB method [Eq. (4)] can also be conducted as

$$\begin{aligned} \tilde{\mathbf{f}}(\mathbf{x} + \mathbf{c}_j \Delta t, t + \Delta t) &= \mathbf{M}^{-1} [\tilde{\mathbf{m}}(\mathbf{x}, t) - \mathbf{S} \tilde{\mathbf{m}}^{ne}(\mathbf{x}, t) \\ &+ \Delta t (\mathbf{m}_G(\mathbf{x}, t) + (\mathbf{I} - \mathbf{S}/2) \mathbf{m}_F(\mathbf{x}, t))], \end{aligned} \quad (57)$$

where $\tilde{\mathbf{f}} = \mathbf{f} - \Delta t \mathbf{F}/2$, $\tilde{\mathbf{m}} = \mathbf{M} \tilde{\mathbf{f}}$, and $\tilde{\mathbf{m}}^{ne} = \tilde{\mathbf{m}} - \mathbf{m}^{eq}$.

From Eqs. (1), (3), and (55)–(57), we can see that there are two ways to analyze and implement the RMRT-LB method: the first one in velocity space and the other in moment space. To recover the NSEs (15) or NCDE (B1) from the RMRT-LB method, one only needs the basic constraints on the functions f_j^{eq} , G_j , and F_j and the collision matrix \mathbf{A} given in Eqs. (17) or (B2). Therefore, using the first way we can analyze the LB models under a unified framework, as shown in Ref. [16]. Compared to the first way, the second one depends on the choice of rDdQq lattice model and the form of the transformation matrix \mathbf{M} , and additionally, the equilibrium moment \mathbf{m}^{eq} also needs to be given properly, which leads to the fact that the modeling and analysis of the MRT-LB models are usually limited to the specified space dimension and lattice structure. This may be one of the main reasons why the RMRT-LB model has not been developed well for a long time. However, the analysis method in moment space enables us to design the equilibrium moment \mathbf{m}^{eq} (e.g., the inverse design of the LB model as in Refs. [24]) more flexibly by selecting the appropriate transformation matrix \mathbf{M} , and the high-order moments which do not influence the recovery of the macroscopic equation(s). If necessary, one can obtain the corresponding EDF f_j^{eq} by taking the inverse transformation (54). It should be noted in this case that the obtained f_j^{eq} may not have the same form as Eqs. (48) or (C1).

Actually, there are still some key questions in the RMRT-LB method. For example, what are the relationships among different forms of collision matrices? How do we choose a proper one? Thanks to the form of the collision matrix in Eq. (52), one can answer the first question, while the second one needs to be further studied.

It is worth noting that the collision matrices in the commonly used MRT-LB method are of the form in Eq. (52) [16], including the raw (natural) moment, cascaded (central-moment), Hermite-moment, and central-Hermite-moment LB models [63,64] with orthogonal and nonorthogonal basis vectors. In fact, any two of the transformation matrices \mathbf{M} and $\bar{\mathbf{M}}$ in these MRT-LB models have the relation,

$$\bar{\mathbf{M}} = \mathbf{N}\mathbf{M}, \quad (58)$$

and one can write the collision matrices with the form in Eq. (52),

$$\mathbf{A} = \bar{\mathbf{M}}^{-1}\bar{\mathbf{S}}\bar{\mathbf{M}} = (\mathbf{N}\mathbf{M})^{-1}\bar{\mathbf{S}}(\mathbf{N}\mathbf{M}) = \mathbf{M}^{-1}\mathbf{S}\mathbf{M}, \quad (59)$$

where \mathbf{N} is a block-lower-triangle matrix, $\mathbf{S} = \mathbf{N}^{-1}\bar{\mathbf{S}}\mathbf{N}$, which means that $\bar{\mathbf{S}}$ is a block-lower-triangle matrix if and only if \mathbf{S} is of the same form. Therefore, the existing MRT-LB models mentioned above can be considered special cases of the present RMRT-LB method. Furthermore, the present RMRT-LB method includes three kinds of MRT-LB models: (1) the popular MRT-LB models on the standard DdQq lattice with $c_s^2 = c^2/3$ [65,66], (2) the MRT-LB models on the standard DdQq lattice with $c_s^2 \neq c^2/3$, and (3) the MRT-LB models on the rectangular rDdQq lattice.

Due to the construction of the relaxation matrix \mathbf{S} in Eq. (52b), and based on Eqs. (58) and (59), we only use the transformation matrix \mathbf{M} related to the raw or natural moments in the analysis and implementation of the RMRT-LB

method,

$$\begin{aligned} \mathbf{m}_{nmp} &= \sum_j c_{jx}^m c_{jy}^n c_{jz}^p f_j, \\ \mathbf{m}_{nmp}^{eq} &= \sum_j c_{jx}^m c_{jy}^n c_{jz}^p f_j^{eq}, \quad m, n, p \in \{0, 1, 2\}, \end{aligned} \quad (60)$$

where $\mathbf{m}_{mn} = \mathbf{m}_{mn0}$ and $\mathbf{m}_{mn}^{eq} = \mathbf{m}_{mn0}^{eq}$ for the two-dimensional case. The transformation matrix \mathbf{M} related to the natural moments in Eq. (60) is composed of $\{c_{jx}^m c_{jy}^n c_{jz}^p, 0 \leq j \leq q-1\}$.

Denoting \mathbf{M} with the following form,

$$\mathbf{M} = (\mathbf{M}_0^T, \mathbf{M}_1^T, \mathbf{M}_2^T, \dots, \mathbf{M}_m^T)^T, \quad \mathbf{M}_k \in \mathbb{R}^{n_k \times q}, \quad 0 \leq k \leq m, \quad (61)$$

then from Eq. (52) we have

$$\mathbf{M}_k \mathbf{A} = \sum_{j=0}^k \mathbf{S}_{kj} \mathbf{M}_j, \quad 0 \leq k \leq m, \quad (62)$$

with the rows corresponding to the zero-, first-, and second-order moments,

$$\begin{aligned} \mathbf{M}_0 &= \mathbf{e} = (1, 1, \dots, 1), \\ \mathbf{M}_1 &= \mathbf{E} = (\mathbf{c}_0, \mathbf{c}_1, \dots, \mathbf{c}_{q-1}), \end{aligned} \quad (63a)$$

$$\begin{aligned} \mathbf{M}_2 &= \begin{pmatrix} \mathbf{M}_2^{(1)} \\ \mathbf{M}_2^{(2)} \end{pmatrix}, \\ S_0 &\in \mathbb{R}, \quad \mathbf{S}_1 \in \mathbb{R}^{d \times d}, \\ \mathbf{S}_2 &\in \mathbb{R}^{\bar{d} \times \bar{d}}, \quad \bar{d} = d(d+1)/2, \end{aligned} \quad (63b)$$

where $\mathbf{M}_2^{(1)} = (\mathbf{c}_{0\alpha} \mathbf{c}_{0\alpha}, \mathbf{c}_{1\alpha} \mathbf{c}_{1\alpha}, \dots, \mathbf{c}_{q-1\alpha} \mathbf{c}_{q-1\alpha})$ and $\mathbf{M}_2^{(2)} = (\mathbf{c}_{0\alpha} \mathbf{c}_{0\beta}, \mathbf{c}_{1\alpha} \mathbf{c}_{1\beta}, \dots, \mathbf{c}_{q-1\alpha} \mathbf{c}_{q-1\beta})_{\alpha < \beta}$. According to Eqs. (30) and (31), we can determine the relaxation submatrix \mathbf{S}_2 as

$$\mathbf{S}_2 = \begin{pmatrix} \bar{\mathbf{S}}_2^{(1)} & 0 \\ 0 & \bar{\mathbf{S}}_2^{(2)} \end{pmatrix}, \quad (64)$$

with

$$\begin{aligned} \bar{\mathbf{S}}_2^{(1)} &= (\mathbf{S}_2^{(1)})^{-1} = \mathbf{A} - \frac{\mathbf{A}\bar{\mathbf{a}}\mathbf{b}^T \mathbf{A}}{1 + \mathbf{b}^T \mathbf{A}\bar{\mathbf{a}}}, \\ \bar{\mathbf{S}}_2^{(2)} &= (\mathbf{S}_2^{(2)})^{-1} = \mathbf{diag}(s_{\alpha\beta})_{\alpha < \beta}, \end{aligned} \quad (65)$$

where $\mathbf{A} = \mathbf{diag}(s_{\alpha\alpha})$, $\bar{\mathbf{a}} = \mathbf{a}/d$, and \mathbf{a} and \mathbf{b} are defined by Eq. (31). Note that the elements $\{s_{\alpha\beta}\}_{\alpha > \beta}$ are not contained in $\bar{\mathbf{S}}_2$ or $(\mathbf{S}_2^{(2)})^{-1}$ since $s_{\alpha\beta} = s_{\beta\alpha}$ for $\alpha \neq \beta$.

For a particular case $\mathbf{S}_{kj} = 0$ ($k > j$), one can obtain

$$\mathbf{S} = \mathbf{diag}(\mathbf{S}_0, \mathbf{S}_1, \dots, \mathbf{S}_m), \quad (66)$$

and Eq. (62) would reduce to

$$\mathbf{M}_k \mathbf{A} = \mathbf{S}_k \mathbf{M}_k, \quad 0 \leq k \leq m, \quad (67)$$

which can be used to derive the commonly used MRT-LB model [3,4].

B. Some special cases of the RMRT-LB method

1. Natural-moment-based RMRT-LB method on rD2Q9 lattice

It should be noted that for the rDdQq lattice, the matrix \mathbf{M} in Eq. (60) can be expressed as $\mathbf{M} = \mathbf{D}\bar{\mathbf{M}}$ with \mathbf{D} being a diagonal matrix. When the discrete velocity set V_q is given,

one can obtain the matrix \mathbf{M} and the other basic components of the RMRT-LB method, such as the collision matrix with proper relaxation matrix, the distribution functions f_j^{eq} , G_j , and F_j , and their moments. We now take the rD2Q9 lattice model [see Eq. (A1)] with the weight coefficients defined by Eqs. (A9) and (A10) as an example, and $\tilde{\mathbf{M}}$, \mathbf{D} , and \mathbf{m}_g^{eq} can be given by

$$\tilde{\mathbf{M}} = \begin{pmatrix} 1 & 1 & 1 & 1 & 1 & 1 & 1 & 1 & 1 \\ 0 & 1 & 0 & -1 & 0 & 1 & -1 & -1 & 1 \\ 0 & 0 & 1 & 0 & -1 & 1 & 1 & -1 & -1 \\ 0 & 1 & 0 & 1 & 0 & 1 & 1 & 1 & 1 \\ 0 & 0 & 1 & 0 & 1 & 1 & 1 & 1 & 1 \\ 0 & 0 & 0 & 0 & 0 & 1 & -1 & 1 & -1 \\ 0 & 0 & 0 & 0 & 0 & 1 & -1 & -1 & 1 \\ 0 & 0 & 0 & 0 & 0 & 1 & 1 & -1 & -1 \\ 0 & 0 & 0 & 0 & 0 & 1 & 1 & 1 & 1 \end{pmatrix}, \quad (68a)$$

$$\mathbf{D} = \text{diag}(1, c_1, c_2, c_1^2, c_2^2, c_1 c_2, c_1 c_2^2, c_1^2 c_2, c_1^2 c_2^2), \quad (68b)$$

$$\mathbf{m}_g^{eq} = \mathbf{M} \mathbf{g}^{eq} = (A, B_x, B_y, c_{s1}^2 A + M_{xx}, c_{s2}^2 A + M_{yy}, M_{xy}, c_{s2}^2 B_x, c_{s1}^2 B_y, c_{s1}^2 c_{s2}^2 A + c_{s2}^2 M_{xx} + c_{s1}^2 M_{yy})^T. \quad (69)$$

The distribution function g_j^{eq} defined by Eq. (44) can be written as

$$g_j^{eq}(A, \mathbf{B}, \mathbf{M}) = \omega_j \left[A + \frac{c_{j\alpha} B_\alpha}{c_{s\alpha}^2} + \frac{M_{xx}(c_{jx}^2 - c_s^2)}{c_{s1}^2(c_1^2 - c_s^2)} + \frac{M_{yy}(c_{jy}^2 - c_s^2)}{c_{s2}^2(c_2^2 - c_s^2)} + \frac{M_{xy}(c_{jx} c_{jy})}{c_{s1}^2 c_{s2}^2} \right]. \quad (70)$$

If we consider the NSEs and take $c_{s1} = c_{s2} = c_s$ in Eqs. (69) and (70), one can obtain f_j^{eq} , G_j , F_j , and their moments from Eqs. (69) and (70),

$$\begin{aligned} f_j^{eq} &= g_j^{eq}(\rho, \rho \mathbf{u}, \rho \mathbf{u} \mathbf{u}) = \rho g_j^{eq}(1, \mathbf{u}, \mathbf{u} \mathbf{u}) \\ &= \omega_j \rho \left[1 + \frac{c_{j\alpha} u_\alpha}{c_s^2} + \frac{u_x^2 (c_{jx}^2 - c_s^2)}{c_s^2 (c_1^2 - c_s^2)} + \frac{u_y^2 (c_{jy}^2 - c_s^2)}{c_s^2 (c_2^2 - c_s^2)} + \frac{u_x u_y c_{jx} c_{jy}}{c_s^4} \right], \end{aligned} \quad (71)$$

$$\begin{aligned} G_j &= g_j^{eq}(0, \mathbf{0}, \mathbf{M}_{2G}) \\ &= \omega_j \left[\frac{\mathbf{M}_{2G,xx}(c_{jx}^2 - c_s^2)}{c_s^2 (c_1^2 - c_s^2)} + \frac{\mathbf{M}_{2G,yy}(c_{jy}^2 - c_s^2)}{c_s^2 (c_2^2 - c_s^2)} + \frac{\mathbf{M}_{2G,xy}(c_{jx} c_{jy})}{c_s^4} \right], \end{aligned} \quad (72)$$

$$\begin{aligned} F_j &= g_j^{eq}(\bar{S}, \bar{\mathbf{F}}, -c_s^2 \bar{S} \mathbf{I}) \\ &= \omega_j \left[\bar{S} + \frac{c_{j\alpha} \bar{F}_\alpha}{c_s^2} - \bar{S} \left(\frac{c_{jx}^2 - c_s^2}{c_1^2 - c_s^2} + \frac{c_{jy}^2 - c_s^2}{c_2^2 - c_s^2} \right) \right], \end{aligned} \quad (73)$$

where \mathbf{M}_{2G} is determined by Eqs. (27) or (51), and

$$\begin{aligned} \mathbf{m}^{eq} &= \mathbf{M} \mathbf{f}^{eq} = \rho (1, u_x, u_y, c_s^2 + u_x^2 + u_y^2 \\ &\quad + u_x^2, u_x u_y, c_s^2 u_x, c_s^2 u_y, c_s^2 (u_x^2 + u_y^2 + c_s^2))^T, \end{aligned} \quad (74)$$

$$\begin{aligned} \mathbf{m}_G &= \mathbf{M} \mathbf{G} = (0, 0, 0, M_{2G,xx}, M_{2G,yy}, M_{2G,xy}, \\ &\quad 0, 0, c_s^2 (M_{2G,xx} + M_{2G,yy}))^T, \end{aligned} \quad (75)$$

$$\mathbf{m}_F = \mathbf{M} \mathbf{F} = (\bar{S}, \bar{F}_x, \bar{F}_y, 0, 0, 0, c_s^2 \bar{F}_x, c_s^2 \bar{F}_y, -c_s^4 \bar{S})^T. \quad (76)$$

For the He-Luo model [17] with $f_j^{eq,HL} = g_j^{eq}(\rho, \rho_0 \mathbf{u}, \rho_0 \mathbf{u} \mathbf{u})$, we have

$$\begin{aligned} \mathbf{m}^{eq,HL} &= \mathbf{M} \mathbf{f}^{eq,HL} \\ &= (\rho, \rho_0 u, \rho_0 v, c_s^2 \rho + \rho_0 u^2, c_s^2 \rho \\ &\quad + \rho_0 v^2, \rho_0 uv, c_s^2 \rho_0 u, c_s^2 \rho_0 v, \\ &\quad c_s^2 (\rho_0 (u^2 + v^2) + c_s^2 \rho))^T, \end{aligned} \quad (77)$$

where $u = u_x$, $v = u_y$.

The relaxation submatrix \mathbf{S}_2 in Eq. (64) and its inverse \mathbf{S}_2^{-1} in Eq. (30) are of the following forms:

$$\mathbf{S}_2 = \begin{pmatrix} \frac{s_{by} + s_{sy}}{s_{by} s_{bx}^{-1} + s_{sy} s_{sx}^{-1}} & \frac{s_{bx} - s_{sx}}{s_{bx} s_{by}^{-1} + s_{sx} s_{sy}^{-1}} \frac{c_1^2 - c_s^2}{c_2^2 - c_s^2} & 0 \\ \frac{s_{by} - s_{sy}}{s_{by} s_{bx}^{-1} + s_{sy} s_{sx}^{-1}} \frac{c_2^2 - c_s^2}{c_1^2 - c_s^2} & \frac{s_{bx} + s_{sx}}{s_{bx} s_{by}^{-1} + s_{sx} s_{sy}^{-1}} & 0 \\ 0 & 0 & s_{xy} \end{pmatrix}, \quad (78a)$$

$$\mathbf{S}_2^{-1} = \begin{pmatrix} \frac{1}{2}(s_{bx}^{-1} + s_{sx}^{-1}) & \frac{1}{2}(s_{bx}^{-1} - s_{sx}^{-1}) \frac{c_1^2 - c_s^2}{c_2^2 - c_s^2} & 0 \\ \frac{1}{2}(s_{by}^{-1} - s_{sy}^{-1}) \frac{c_2^2 - c_s^2}{c_1^2 - c_s^2} & \frac{1}{2}(s_{by}^{-1} + s_{sy}^{-1}) & 0 \\ 0 & 0 & s_{xy}^{-1} \end{pmatrix}. \quad (78b)$$

In addition, it follows from Eq. (33) that

$$\begin{aligned} (s_{bx}^{-1} - s_{sx}^{-1})(c_1^2 - c_s^2) &= (s_{by}^{-1} - s_{sy}^{-1})(c_2^2 - c_s^2), \quad (79a) \\ (s_{bx}^{-1} + s_{sx}^{-1} - 1)(c_1^2 - c_s^2) &= (s_{by}^{-1} + s_{sy}^{-1} - 1)(c_2^2 - c_s^2). \end{aligned} \quad (79b)$$

Then \mathbf{S}_2^{-1} in Eq. (78b) becomes

$$\mathbf{S}_2^{-1} = \begin{pmatrix} \frac{1}{2}(s_{bx}^{-1} + s_{sx}^{-1}) & \frac{1}{2}(s_{bx}^{-1} - s_{sx}^{-1}) \frac{c_1^2 - c_s^2}{c_2^2 - c_s^2} & 0 \\ \frac{1}{2}(s_{bx}^{-1} - s_{sx}^{-1}) & \frac{1}{2}(s_{bx}^{-1} + s_{sx}^{-1}) \frac{c_1^2 - c_s^2}{c_2^2 - c_s^2} + \frac{1}{2} \frac{c_2^2 - c_s^2}{c_1^2 - c_s^2} & 0 \\ 0 & 0 & s_{xy}^{-1} \end{pmatrix}. \quad (80)$$

Note that to recover correct macroscopic equation(s), only some basic constraints are needed, which means that for NSEs, the fourth-order moment of f_j^{eq} , the third- and fourth-order moments of G_j , and the second- to fourth-order moments of F_j can be taken as any values. Once these moments are specified, the distribution functions can be obtained by $\mathbf{f}^{eq} = \mathbf{M}^{-1} \mathbf{m}^{eq}$, $\mathbf{G} = \mathbf{M}^{-1} \mathbf{m}_G$, and $\mathbf{F} = \mathbf{M}^{-1} \mathbf{m}_F$.

2. Hermite-moment-based RMRT-LB method on the rD2Q9 lattice

Based on the transformation matrix \mathbf{M} related to the natural moment, given the matrix $\mathbf{N} = \mathbf{N}_H$ as in Eq. (58) such

that $\mathbf{M}_H = \mathbf{N}_H \mathbf{M}$, one can obtain the Hermite-moment-based RMRT-LB model with collision matrix $\mathbf{\Lambda} = \mathbf{M}_H^{-1} \mathbf{S}_H \mathbf{M}_H =$

$\mathbf{M}^{-1} \mathbf{S} \mathbf{M}$ with $\mathbf{S} = \mathbf{N}_H^{-1} \mathbf{S}_H \mathbf{N}_H$. For the rD2Q9 lattice model, the matrix \mathbf{N}_H can be given by

$$\mathbf{N}_H = \begin{pmatrix} 1 & 0 & 0 & 0 & 0 & 0 & 0 & 0 & 0 \\ 0 & 1 & 0 & 0 & 0 & 0 & 0 & 0 & 0 \\ 0 & 0 & 1 & 0 & 0 & 0 & 0 & 0 & 0 \\ -c_{s1}^2 & 0 & 0 & 1 & 0 & 0 & 0 & 0 & 0 \\ -c_{s2}^2 & 0 & 0 & 0 & 1 & 0 & 0 & 0 & 0 \\ 0 & 0 & 0 & 0 & 0 & 1 & 0 & 0 & 0 \\ 0 & -c_{s2}^2 & 0 & 0 & 0 & 0 & 1 & 0 & 0 \\ 0 & 0 & -c_{s1}^2 & 0 & 0 & 0 & 0 & 1 & 0 \\ c_{s1}^2 c_{s2}^2 & 0 & 0 & -c_{s2}^2 & -c_{s1}^2 & 0 & 0 & 0 & 1 \end{pmatrix}. \quad (81)$$

From the expression of \mathbf{N}_H , it is easy to find that the diagonal elements in the relaxation matrices \mathbf{S}_H and \mathbf{S} are the same as each other. With the help of the transformation matrix \mathbf{M}_H , the moments of g_j^{eq} in Eq. (70) can be determined by

$$\mathbf{m}_g^{eq,H} = \mathbf{M}_H \mathbf{g}^{eq} = \mathbf{N}_H \mathbf{m}_g^{eq} = (A, B_x, B_y, M_{xx}, M_{yy}, M_{xy}, 0, 0, 0)^T. \quad (82)$$

3. Central-moment-based RMRT-LB method for NSEs on rD2Q9 lattice

Similarly, one can obtain the central-moment-based RMRT-LB model with collision matrix $\mathbf{\Lambda} = \mathbf{M}_C^{-1} \mathbf{S}_C \mathbf{M}_C = \mathbf{M}^{-1} \mathbf{S} \mathbf{M}$ with $\mathbf{M}_C = \mathbf{N}_C \mathbf{M}$, $\mathbf{S} = \mathbf{N}_C^{-1} \mathbf{S}_C \mathbf{N}_C$. For the rD2Q9 lattice model, the expression of \mathbf{N}_C can be given as

$$\mathbf{N}_C = \begin{pmatrix} 1 & 0 & 0 & 0 & 0 & 0 & 0 & 0 & 0 \\ -u & 1 & 0 & 0 & 0 & 0 & 0 & 0 & 0 \\ -v & 0 & 1 & 0 & 0 & 0 & 0 & 0 & 0 \\ u^2 & -2u & 0 & 1 & 0 & 0 & 0 & 0 & 0 \\ v^2 & 0 & -2v & 0 & 1 & 0 & 0 & 0 & 0 \\ uv & -v & -u & 0 & 0 & 1 & 0 & 0 & 0 \\ -uv^2 & v^2 & 2uv & 0 & -u & -2v & 1 & 0 & 0 \\ -u^2v & 2uv & u^2 & -v & 0 & -2u & 0 & 1 & 0 \\ u^2v^2 & -2uv^2 & -2u^2v & v^2 & u^2 & 4uv & -2u & -2v & 1 \end{pmatrix}. \quad (83)$$

Furthermore, the central-Hermite-moment-based RMRT-LB model with collision matrix $\mathbf{\Lambda} = \mathbf{M}_{HC}^{-1} \mathbf{S}_{HC} \mathbf{M}_{HC} = \mathbf{M}^{-1} \mathbf{S} \mathbf{M}$ can be obtained by the combination of Hermite-moment- and central-moment-based RMRT-LB models in which $\mathbf{M}_{HC} = \mathbf{N}_{HC} \mathbf{M}$, $\mathbf{S} = \mathbf{N}_{HC}^{-1} \mathbf{S}_{HC} \mathbf{N}_{HC}$, and $\mathbf{N}_{HC} = \mathbf{N}_H \mathbf{N}_C$. From the forms of \mathbf{N}_C and \mathbf{N}_H one can also find that the relaxation matrices \mathbf{S}_C , \mathbf{S}_{HC} , and \mathbf{S} have the same diagonal elements.

4. The RMRT-LB model for NSEs in Reference [34]

It can also be found that the orthogonal transformation matrix \mathbf{M}_{ZKA} based on the rD2Q9 and rD3Q27 lattices in Ref. [34] have the form of $\mathbf{M}_{ZKA} = \mathbf{N}_{ZKA} \mathbf{M}$ with \mathbf{N}_{ZKA} being a lower-triangular matrix, and \mathbf{m}_{ZKA}^{eq} in Ref. [34] can also be obtained,

$$\mathbf{m}_{ZKA}^{eq} = \mathbf{M}_{ZKA} \mathbf{f}^{eq} = \mathbf{N}_{ZKA} \mathbf{m}^{eq}, \quad (84)$$

with parameters $\gamma_2 = \gamma_5 = \gamma_7 = c_s^4$, $\gamma_3 = \gamma_4 = c_s^2$, $\gamma_6 = c_s^6$. Then we have

$$\mathbf{N}_{ZKA} = \begin{pmatrix} 1 & 0 & 0 & 0 & 0 & 0 & 0 & 0 & 0 \\ 0 & 1 & 0 & 0 & 0 & 0 & 0 & 0 & 0 \\ 0 & 0 & 1 & 0 & 0 & 0 & 0 & 0 & 0 \\ -2c_1^2 & 0 & 0 & 3 & 0 & 0 & 0 & 0 & 0 \\ -2c_2^2 & 0 & 0 & 0 & 3 & 0 & 0 & 0 & 0 \\ 0 & 0 & 0 & 0 & 0 & 1 & 0 & 0 & 0 \\ 0 & -2c_2^2 & 0 & 0 & 0 & 0 & 3 & 0 & 0 \\ 0 & 0 & -2c_1^2 & 0 & 0 & 0 & 0 & 3 & 0 \\ 4c_1^2 c_2^2 & 0 & 0 & -6c_2^2 & -6c_1^2 & 0 & 0 & 0 & 9 \end{pmatrix}, \quad (85)$$

$$\mathbf{m}_{ZKA}^{eq} = \rho(1, u, v, 3(c_s^2 + u^2) - 2c_1^2, 3(c_s^2 + v^2) - 2c_2^2, uv, u(3c_s^2 - 2c_2^2), v(3c_s^2 - 2c_1^2), C)^T, \quad (86)$$

where $C = 9c_s^2(c_s^2 + u^2 + v^2) + 4c_1^2 c_2^2 - 6c_2^2(u^2 + c_s^2) - 6c_1^2(v^2 + c_s^2)$ is the fourth-order moment of equilibrium, while the first term of C has a more general form $9[\gamma_2 + \gamma_3(u^2 + v^2)]$ in Ref. [34], and the parameters γ_2 and γ_3 can be set by any values, which

does not affect the correct recovery of the NSEs. \mathbf{N}_{ZKA} has the same structure as \mathbf{N}_H in Eq. (81), and the diagonal elements in the relaxation matrices \mathbf{S}_{ZKA} and \mathbf{S} are the same; thus Eqs. (33) or (36) is satisfied for the transformation matrices of the natural moment and the orthogonal one in Ref. [34]. However, \mathbf{S}_{ZKA} is diagonal, which means that the bulk viscosity is not considered in Ref. [34]. In addition, due to the fact that there is no orthogonal transformation matrix for rD3Q19, as stated in Ref. [34], the RMRT-LB model with rD3Q19 lattice cannot be given [34], while the present RMRT-LB model with rD3Q19 lattice is ready at hand.

5. RMRT-LB models for the NSEs in References [27,28]

The relationship between the matrix \mathbf{M} in Eq. (60) and those in Refs. [27,28] is interesting. Let $c_1 = 1$ and $c_2 = a$ in Eq. (68b). The matrix \mathbf{M} determined by Eq. (68) becomes

$$\mathbf{M}_a = \mathbf{D}_a \tilde{\mathbf{M}} = \begin{pmatrix} 1 & 1 & 1 & 1 & 1 & 1 & 1 & 1 & 1 \\ 0 & 1 & 0 & -1 & 0 & 1 & -1 & -1 & 1 \\ 0 & 0 & a & 0 & -a & a & a & -a & -a \\ 0 & 1 & 0 & 1 & 0 & 1 & 1 & 1 & 1 \\ 0 & 0 & a^2 & 0 & a^2 & a^2 & a^2 & a^2 & a^2 \\ 0 & 0 & 0 & 0 & 0 & a & -a & a & -a \\ 0 & 0 & 0 & 0 & 0 & a^2 & -a^2 & -a^2 & a^2 \\ 0 & 0 & 0 & 0 & 0 & a & a & -a & -a \\ 0 & 0 & 0 & 0 & 0 & a^2 & a^2 & a^2 & a^2 \end{pmatrix}, \tag{87a}$$

$$\mathbf{D}_a = \text{diag}(1, 1, a, 1, a^2, a, a^2, a, a^2), \tag{87b}$$

and the orthogonal transformation matrix used in Ref. [27] can be written as

$$\mathbf{M}_{BHLL} = \mathbf{N}_{BHLL} \mathbf{M}_a = \begin{pmatrix} 1 & 1 & 1 & 1 & 1 & 1 & 1 & 1 & 1 \\ 0 & 1 & 0 & -1 & 0 & 1 & -1 & -1 & 1 \\ 0 & 0 & a & 0 & -a & a & a & -a & -a \\ -2r_1 & r_2 & r_3 & r_2 & r_3 & r_1 & r_1 & r_1 & r_1 \\ -2r_4 & r_5 & r_6 & r_5 & r_6 & r_4 & r_4 & r_4 & r_4 \\ 0 & 0 & 0 & 0 & 0 & a & -a & a & -a \\ 0 & -2 & 0 & 2 & 0 & 1 & -1 & -1 & 1 \\ 0 & 0 & -2a & 0 & 2a & a & a & -a & -a \\ 4 & -2 & -2 & -2 & -2 & 1 & 1 & 1 & 1 \end{pmatrix}, \tag{88a}$$

where

$$r_1 = 1 + a^2, \quad r_2 = 1 - 2a^2, \quad r_3 = -2 + a^2, \quad r_4 = -1 + a^2, \quad r_5 = 2 + a^2, \quad r_6 = -1 - 2a^2, \tag{88b}$$

$$\mathbf{N}_{BHLL} = \begin{pmatrix} 1 & 0 & 0 & 0 & 0 & 0 & 0 & 0 & 0 \\ 0 & 1 & 0 & 0 & 0 & 0 & 0 & 0 & 0 \\ 0 & 0 & 1 & 0 & 0 & 0 & 0 & 0 & 0 \\ -2a^2 - 2 & 0 & 0 & 3 & 3 & 0 & 0 & 0 & 0 \\ -2a^2 + 2 & 0 & 0 & 3a^2 & -3/a^2 & 0 & 0 & 0 & 0 \\ 0 & 0 & 0 & 0 & 0 & 1 & 0 & 0 & 0 \\ 0 & -2 & 0 & 0 & 0 & 0 & 3/a^2 & 0 & 0 \\ 0 & 0 & -2 & 0 & 0 & 0 & 0 & 3 & 0 \\ 4 & 0 & 0 & -6 & -6/a^2 & 0 & 0 & 0 & 9/a^2 \end{pmatrix}. \tag{89}$$

In addition, the related equilibrium moments can be obtained,

$$\begin{aligned} \mathbf{m}_{BHLL}^{eq} &= \mathbf{M}_{BHLL} \mathbf{f}^{eq} = \mathbf{N}_{BHLL} \mathbf{M} \mathbf{f}^{eq} = \rho(1, u, v, \bar{e}^{eq}, \bar{p}_{xx}^{eq}, uv, C_1 u/2, C_2 v/2, C_3)^T, \\ \bar{e}^{eq} &= 3(u^2 + v^2) + 2(3c_s^2 - r_1), \quad \bar{p}_{xx}^{eq} = r_4(3r_1 c_s^2 - 2a^2)/a^2 + 3(a^2 u^2 - v^2/a^2), \end{aligned} \tag{90}$$

with

$$C_1 = 2(3c_s^2 - 2a^2)/a^2, \quad C_2 = 2(3c_s^2 - 2), \quad C_3 = (9c_s^4 + 9c_s^2 u^2 + 9c_s^2 v^2 - 6c_s^2 - 6v^2)/a^2 - (6u^2 + 6c_s^2 - 4). \tag{91}$$

Note that C_1 and C_2 satisfy the relation

$$C_1 = [C_2 + 4(1 - a^2)]/a^2, \quad (92)$$

which is the same as that in Ref. [27]. When C_1 and C_2 are taken by Eq. (91), one can find that the equilibrium moments in Eq. (90) are the same as those in Ref. [27] except for the fourth-order moment ε^{eq} which does not affect the correct recovery of the NSEs. This implies that for the RMRT-LB model in Ref. [27], one can correctly recover the NSEs (15) when the relaxation submatrix \mathbf{S}_2^{-1} in Eqs. (78b) or (80) is adopted. In other words, if the diagonal relaxation submatrix $\mathbf{S}_{2,BHLL}^{-1} = \mathbf{diag}(\bar{s}_4^{-1}, \bar{s}_5^{-1}, \bar{s}_6^{-1})$ in Ref. [27] is modified by $\bar{\mathbf{S}}_2^{-1} = \mathbf{N}_{2,BHLL} \mathbf{S}_2^{-1} \mathbf{N}_{2,BHLL}^{-1}$, the NSEs can be recovered correctly from the RMRT-LB model in Ref. [27]. Here $\mathbf{N}_{2,BHLL}$ is the diagonal subblock of \mathbf{N}_{BHLL} corresponding to the second-order moment,

$$\mathbf{N}_{2,BHLL} = \begin{pmatrix} 3 & 3 & 0 \\ 3a^2 & -3/a^2 & 0 \\ 0 & 0 & 1 \end{pmatrix}, \quad (93)$$

and \bar{s}_4, \bar{s}_5 , and \bar{s}_6 are s_2, s_8 , and s_9 in Ref. [27]. One can also easily obtain

$$\begin{aligned} \bar{\mathbf{S}}_2^{-1} &= \mathbf{N}_{2,BHLL} \mathbf{S}_2^{-1} \mathbf{N}_{2,BHLL}^{-1} \\ &= \frac{1}{1+a^4} \begin{pmatrix} A_1 & A_2 & 0 \\ A_3 & A_4 & 0 \\ 0 & 0 & (1+a^4)s_{xy}^{-1} \end{pmatrix}, \end{aligned} \quad (94)$$

$$\bar{\mathbf{S}}_2^{-1} = \mathbf{N}_{2,BHLL} \mathbf{S}_2^{-1} \mathbf{N}_{2,BHLL}^{-1} = \frac{1}{1+a^4} \begin{pmatrix} s_{sx}^{-1} + a^4 s_{sy}^{-1} & a^2 (s_{sx}^{-1} - s_{sy}^{-1}) & 0 \\ a^2 (s_{sx}^{-1} - s_{sy}^{-1}) & a_4 s_{sx}^{-1} + s_{sy}^{-1} & 0 \\ 0 & 0 & (1+a^4)s_{xy}^{-1} \end{pmatrix}, \quad (97)$$

which is not diagonal for the case $a \neq 1$ due to $s_{sx} \neq s_{sy}$ on the rD2Q9 lattice. Furthermore, one can transform $\bar{\mathbf{S}}_2^{-1}$ in Eq. (97) into a diagonal matrix by changing \mathbf{N}_{BHLL} or $\mathbf{N}_{2,BHLL}$. Following the idea in Ref. [28], we modified \mathbf{N}_{BHLL} as \mathbf{N}_{ZPGW} ,

$$\mathbf{N}_{ZPGW} = \begin{pmatrix} 1 & 0 & 0 & 0 & 0 & 0 & 0 & 0 & 0 \\ 0 & 1 & 0 & 0 & 0 & 0 & 0 & 0 & 0 \\ 0 & 0 & 1 & 0 & 0 & 0 & 0 & 0 & 0 \\ 0 & 0 & 0 & 1 & \theta & 0 & 0 & 0 & 0 \\ 0 & 0 & 0 & -\theta & 1 & 0 & 0 & 0 & 0 \\ 0 & 0 & 0 & 0 & 0 & 1 & 0 & 0 & 0 \\ 0 & 0 & 0 & 0 & 0 & 0 & 1 & 0 & 0 \\ 0 & 0 & 0 & 0 & 0 & 0 & 0 & 1 & 0 \\ 0 & 0 & 0 & 0 & 0 & 0 & 0 & 0 & 1 \end{pmatrix} \mathbf{N}_{BHLL}, \quad (98)$$

with

$$\begin{aligned} \mathbf{N}_{2,ZPGW} &= \begin{pmatrix} 1 & \theta & 0 \\ -\theta & 1 & 0 \\ 0 & 0 & 1 \end{pmatrix} \\ \mathbf{N}_{2,BHLL} &= \begin{pmatrix} 3(1+a^2\theta) & 3(1-\theta/a^2) & 0 \\ 3(a^2-\theta) & -3(\theta+1/a^2) & 0 \\ 0 & 0 & 1 \end{pmatrix}, \end{aligned} \quad (99)$$

where θ is a parameter to be determined, and $\mathbf{M}_{ZPGW} = \mathbf{N}_{ZPGW} \mathbf{M}$ is still orthogonal. It can be

where

$$\begin{aligned} A_1 &= (a_1 + a_2)(1 + a^4 A) + a^4(1 - A)/2, \\ A_2 &= a^2(1 - A)(a_1 + a_2 - 1/2), \end{aligned} \quad (95a)$$

$$\begin{aligned} A_3 &= a^2(1 - A)(a_1 - 1/2) + (Aa^8 - 1)a_2/a^2, \\ A_4 &= a_1(A + a^4) - a_2(1 + Aa^4) + (1 - A)/2, \end{aligned} \quad (95b)$$

with

$$\begin{aligned} a_1 &= \frac{1}{2}(s_{bx} + s_{sx}), \quad a_2 = \frac{1}{2}(s_{bx} - s_{sx}), \\ A &= \frac{c_1^2 - c_s^2}{c_2^2 - c_s^2} = \frac{1 - c_s^2}{a^2 - c_s^2}. \end{aligned} \quad (96)$$

It is clear that due to $a_1 + a_2 = s_{bx}^{-1} > 1/2$, $\bar{\mathbf{S}}_2^{-1}$ is diagonal if and only if $A = 1$ and $a = 1$, which means that $\bar{\mathbf{S}}_2^{-1} = \mathbf{S}_{2,BHLL}^{-1}$ holds only on the square lattice with $s_{bx} = s_{by} = \bar{s}_4$, $s_{sx} = s_{sy} = \bar{s}_5$, and $s_{xy} = \bar{s}_6$. Therefore, if we use the diagonal subrelaxation matrix $\mathbf{S}_{2,BHLL}^{-1}$ instead of $\bar{\mathbf{S}}_2^{-1}$ in Eq. (94), the RMRT-LB model in Ref. [27] cannot correctly recover the NSEs unless $a = 1$. It should be noted that $\bar{\mathbf{S}}_2^{-1}$ in Eq. (94) has a complicated form when using the orthogonal transformation matrix \mathbf{M}_{BHLL} . However, if we take $s_{bx} = s_{sx}$ and $s_{by} = s_{sy}$ in Eq. (78b) for the incompressible or weakly compressible NSEs, $\mathbf{S}_2^{-1} = \mathbf{diag}(s_{sx}^{-1}, s_{sy}^{-1}, s_{xy}^{-1})$ becomes diagonal, and then one can obtain a simpler $\bar{\mathbf{S}}_2^{-1}$ form of Eqs. (79b) and (94),

easily shown that $\theta = a^2$ or $\theta = -a^{-2}$ if and only if $\mathbf{N}_{2,ZPGW}^{-1} \mathbf{S}_2^{-1} \mathbf{N}_{2,ZPGW} = \mathbf{diag}(s_{sx}^{-1}, s_{sy}^{-1}, s_{xy}^{-1}) = \mathbf{S}_2^{-1}$ or $\mathbf{N}_{2,ZPGW}^{-1} \mathbf{S}_2^{-1} \mathbf{N}_{2,ZPGW} = \mathbf{diag}(s_{sy}^{-1}, s_{sx}^{-1}, s_{xy}^{-1})$. The RMRT-LB model for the NSEs similar to that in Ref. [28] is directly obtained in a much simpler way from our general framework where there are no any limitations on θ .

V. NUMERICAL RESULTS AND DISCUSSIONS

To test the present RMRT-LB method, a two-dimensional (2D) convection-diffusion equation (CDE) and a 2D lid-driven cavity flow are considered in this section. In the simulations, we use the collision matrix $\mathbf{\Lambda} = \mathbf{M}^{-1} \mathbf{S} \mathbf{M}$ with the transformation matrix \mathbf{M} related to the natural moments, the relaxation matrix $\mathbf{S} = \mathbf{diag}\{s_0, s_1, s_2, s_3, s_4, s_5, s_6, s_7, s_8\}$ is diagonal for both the CDE and NSEs, and the distribution function f_j is initialized by its equilibrium distribution function f_j^{eq} . In addition, some parameters are set to be $c_1 = 1$, $c_2/c_1 = a$, and $c_s^2 = c_1^2 d_{01} = c_2^2 d_{02} = d_{01}$.

A. The 2D convection-diffusion equation

Here we consider a two-dimensional isotropic CDE with a constant velocity, which is given by

$$\partial_t \phi + u_x \partial_x \phi + u_y \partial_y \phi = \kappa (\partial_{xx} \phi + \partial_{yy} \phi) + S, \quad (100)$$

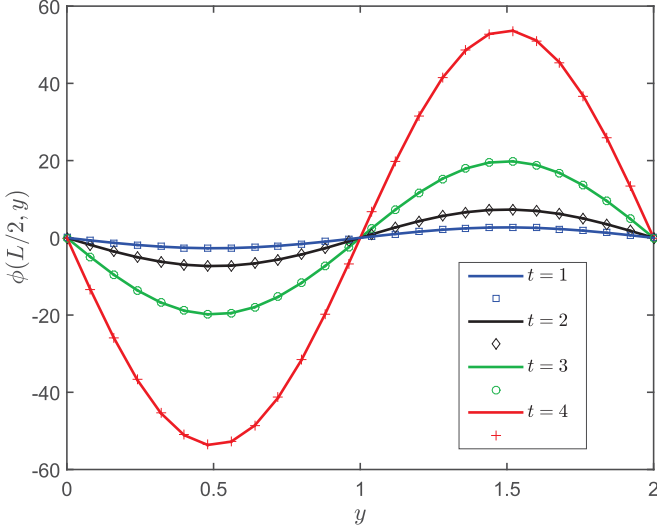


FIG. 1. Profiles of scalar variable ϕ at different times and $Pe = 1000$. The solid lines and symbols represent analytical solutions and numerical results, respectively.

where u_x and u_y are constants and $u_x = u_y$. κ is the diffusion coefficient with $\kappa = c_s^2(\tau - 0.5)\Delta t$. S is the source term which can be expressed as

$$S = \exp[(1 - 2\pi^2\kappa)t] \{ \sin[\pi(x+y)] + \pi(u_x + u_y) \cos[\pi(x+y)] \}. \quad (101)$$

In our simulations, the Péclet number ($Pe = Lu_x/\kappa$, $L = 2.0$ is characteristic length, u_x is characteristic velocity) is chosen as $Pe = 100, 1000$, and the relaxation parameters are set to be $s_1 = s_2 = 1/\tau$, $s_0 = s_3 = s_4 = s_5 = s_6 = s_7 = s_8 = 1.0$. The computational domain is $[0, 2] \times [0, 2]$, the periodic boundary condition, and the following initial condition are adopted:

$$\phi(x, y, t = 0) = \sin[\pi(x+y)]. \quad (102)$$

In addition, Eqs. (1) or (56) with $\gamma = 0$ is used for solving Eq. (100), where $f_j^{eq} = \phi g_j^{eq}(1, \mathbf{u}, \mathbf{uu})$, $\mathbf{M}_{1G} = (1 - s_1/2)\mathbf{S}\mathbf{u}$, $\mathbf{u} = (u_x, u_y)$ in Eqs. (C1) and (C2). For this problem, one can derive the following analytical solution:

$$\phi_a(x, y, t) = \exp[(1 - 2\pi^2\kappa)t] \sin[\pi(x+y)]. \quad (103)$$

Here, the following global relative error (GRE) is used to test the accuracy of the present RMRT-LB method:

$$\text{Err} = \frac{\sum_{\mathbf{x}} |\phi_a(x, y, t) - \phi_n(x, y, t)|}{\sum_{\mathbf{x}} |\phi_a(x, y, t)|}, \quad (104)$$

where the subscripts a and n denote the analytical and numerical solutions. As seen from Fig. 1, the numerical results are in good agreement with analytical solutions at $t = 1, 2, 3$, and 4 . To give a more detailed comparison, we also performed some simulations with different times ($t_1 = 2$ and $t_2 = 10$), different meshes, and different parameters a and c_s^2 (or d_{01} and d_{02}), and presented the results in Tables I and II. From these two tables, one can observe that global relative errors are about $O(10^{-4})$, which is very close to the results in Ref. [39]. It is also found that the choice of c_s could affect the numerical results. We noted that, even for a small grid aspect ratio $a = 0.1$, the present method can produce accurate results. In addition, we would like to point out that when Pe is sufficiently large, e.g., $Pe = 10^9$, τ is very close to 0.5 , and the GRE remains on the order of 10^{-4} , which indicates that the present RMRT-LB method has good numerical stability and accuracy.

B. The 2D lid-driven cavity flow

To demonstrate the capability of the current RMRT-LB method in the study of fluid flows, we carried out some simulations of the two-dimensional lid-driven cavity flows. Although the geometry of the problem is very simple, the lid-driven cavity flow is of great scientific interest because it displays rich fluid mechanical phenomena, especially complex vortex dynamics. We consider a square cavity of side $H = 1.0$ and top wall with a constant velocity U , and this problem is characterized by the dimensionless Reynolds number which can be defined as $Re = UH/\nu$. In this test, we first carried out simulations with $Re = 1000$ and a wide range of grid aspect ratios of $4, 2, 0.5$, and 0.2 . The relaxation parameters are set to be $s_0 = s_1 = s_2 = 1.0$, $s_3 = 1/\tau_x$, $s_4 = 1/\tau_y$, $s_5 = 1/\tau$, and $s_6 = s_7 = s_8 = 1.0$, and the other parameters are given in Table III. In addition, the nonequilibrium extrapolation scheme is adopted to treat physical boundary conditions [67]. Figure 2 shows the velocity profiles along the vertical and horizontal centerlines at $Re = 1000$ and $a = 4, 2, 0.5$, and 0.2 . From this figure, one can observe that the present results agree well with those reported in Ref. [68], which means that the present RMRT-LB method can give accurate results for a wide range of grid aspect ratios.

TABLE I. The global relative errors at different parameters and $Pe = 100$.

a	$Nx \times Ny$	u_x	κ	c_s^2	d_{02}	$\tau = 1/s_1$	$\text{Err}_{-t_1} (\times 10^{-4})$	$\text{Err}_{-t_2} (\times 10^{-4})$
2	100 × 50	0.1	2×10^{-3}	0.333	0.083	0.8	8.3104	8.2754
				0.2	0.05	1.0	5.2749	5.4581
1	100 × 100	0.1	2×10^{-3}	0.333	0.333	0.8	8.7246	8.8302
				0.2	0.2	1.0	4.4420	4.5940
0.8	100 × 125	0.1	2×10^{-3}	0.333	0.52	0.8	8.0818	8.9251
				0.2	0.3125	1.0	4.7135	4.8751
0.5	50 × 100	0.1	2×10^{-3}	0.05	0.2	1.5	4.0012	4.7679
0.2	50 × 250	0.01	2×10^{-4}	0.005	0.125	1.5	5.8079	6.0628
0.1	50 × 500	0.01	2×10^{-4}	0.005	0.5	1.5	5.0802	6.0537

TABLE II. The global relative errors (GREs) with different parameters at $Pe = 1000$.

a	$N_x \times N_y$	u_x	κ	c_s^2	d_{02}	$\tau = 1/s_1$	$Err_{f_1} (\times 10^{-4})$	$Err_{f_2} (\times 10^{-4})$
2	100×50	0.1	2×10^{-4}	0.333	0.083	0.53	9.5243	9.8073
				0.05	0.0125	0.7	2.4966	2.5395
1	100×100	0.1	2×10^{-4}	0.333	0.333	0.53	8.6231	8.6742
				0.05	0.05	0.7	2.5548	2.6274
0.8	100×125	0.1	2×10^{-4}	0.333	0.52	0.53	8.5365	8.5587
				0.05	0.078	0.7	2.5701	2.6465
0.2	50×250	0.01	2×10^{-5}	0.005	0.125	0.6	6.0960	6.9829
0.1	50×500	0.01	2×10^{-5}	0.005	0.5	0.6	6.0951	6.9822
				0.01	1.0	0.55	6.5144	7.4039

TABLE III. The parameters adopted in the simulation of lid-driven cavity flow at $Re = 1000$.

a	$N_x \times N_y$	U	c_s^2	d_{02}	$\tau = 1/s_5$	$\tau_x = 1/s_3$	$\tau_y = 1/s_4$	ν
4	200×50	0.1	1/3	1/48	0.56	0.56	0.5026	0.0001
2	200×100	0.1	1/3	1/12	0.56	0.56	0.5109	0.0001
0.5	200×400	0.05	1/12	1/3	0.62	0.5218	0.62	0.00005
0.2	100×500	0.02	0.02	0.5	0.6	0.5041	0.7	0.00002

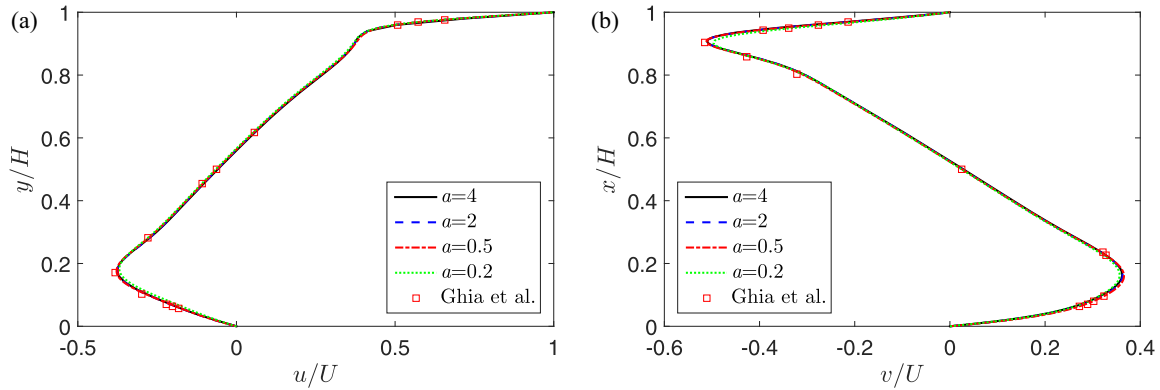


FIG. 2. Velocity profiles along centerlines at different aspect ratios: (a) u along the vertical centerline and (b) v along the horizontal centerline.

TABLE IV. The parameters adopted in the simulation of lid-driven cavity flow.

Re	a	$N_x \times N_y$	U	c_s^2	d_{02}	$\tau = 1/s_5$	$\tau_x = 1/s_3$	$\tau_y = 1/s_4$	ν
1000	0.5	200×400	0.05	1/12	1/3	0.62	0.5218	0.62	0.00005
3200	0.5	300×600	0.05	0.08	0.32	0.5586	0.5102	0.5551	0.000016
5000	0.5	300×600	0.05	0.05	0.2	0.56	0.5063	0.53	0.00001

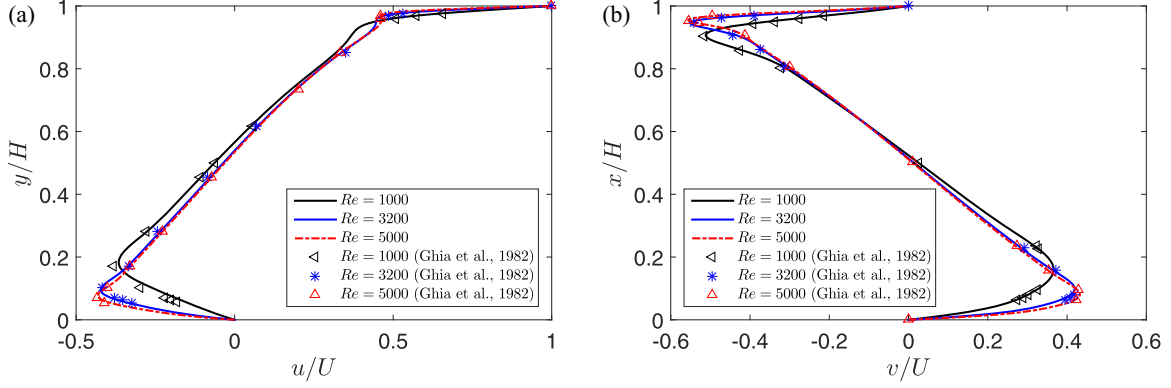


FIG. 3. A comparison of velocity profiles along the centerlines between the present work and Ghia *et al.* [68]: (a) u along the vertical centerline and (b) v along the horizontal centerline.

We note that although some rectangular LB models based on either SRT or orthogonal MRT formulations have been used to simulate this problem [24,27–29], they are usually subjected to a numerical instability issue when Re is increased to a moderate value [32]. To test the numerical stability of the present RMRT-LB model, we conducted some simulations at $Re = 1000, 3200$, and 5000 and $a = 0.5$. The parameters are shown in Table IV. Figure 3 depicts the velocity profiles along the vertical and horizontal centerlines at $Re = 1000, 3200$, and 5000 , from which we can see that the present results agree well with those of Ghia *et al.* [68]. This example also shows that the current RMRT-LB method still has good numerical stability at relatively large Reynolds numbers.

VI. CONCLUSIONS

Following recent work [16], we developed a general framework of the RMRT-LB method on the $rDdQq$ lattice for the NSEs and NCDE, in which a block-lower-triangular-relaxation matrix is used. The modeling and analysis approaches adopt the same idea as those for the SRT-LB model in which only the distribution function space and some basic moment conditions of distribution function are considered;

thus the current RMRT-LB method is more natural. We conducted a detailed DTE analysis on the present RMRT-LB method, and the NSEs can be correctly recovered, while the analysis of the RMRT-LB method for NCDE is omitted since it is the same as that in Ref. [16]. Then the rectangular $rDdQq$ lattice models, the properties of velocity moments, and the expression of weight coefficients are discussed, and a general quadratic EDF is obtained based on the previous work [35]. After that, the EDFs satisfying the basic moment conditions for NSEs and NCDE are given, respectively. Furthermore, the structure of the collision matrix in the RMRT-LB method is analyzed, and it is found that some existing MRT-LB models can be viewed as special cases of the present RMRT-LB method, including the classical MRT-LB model, central-moment LB model, and Hermite-moment and central-Hermite-moment LB models. In addition, two versions of those MRT-LB models with third-order anisotropic moments, one on a standard $DdQq$ lattice with $c_s^2 \neq c^2/3$ [17,36–38] and the other on a rectangular $rDdQq$ lattice [34], are also two special cases of the present RMRT-LB method. Two examples, including a convection-diffusion equation and a lid-driven cavity flow, are used to test the present RMRT-LB method, and the results indicate that the present method has good numerical accuracy and stability.

ACKNOWLEDGMENT

This work was financially supported by the National Natural Science Foundation of China (Grants No. 12072127, No. 51836003, and No. 12202130).

APPENDIX A: LATTICE MODELS OF THE RMRT-LB METHOD ON A RECTANGULAR LATTICE

In this Appendix, we focus on the $rDdQq$ lattice models. To simplify the following analysis, we introduce $c_\alpha = \Delta x_\alpha / \Delta t$ ($\alpha = 1, 2, \dots, d$) in d -dimensional space with Δx_α being the spacing step in the α axis. In this case, the discrete velocities and weight coefficients in the common $rDdQq$ lattice models can be given as follows.

For the $rD2Q9$ lattice,

$$\{\mathbf{c}_j, 0 \leq j \leq 8\} = \begin{pmatrix} 0 & c_1 & 0 & -c_1 & 0 & c_1 & -c_1 & -c_1 & c_1 \\ 0 & 0 & c_2 & 0 & -c_2 & c_2 & c_2 & -c_2 & -c_2 \end{pmatrix},$$

$$\omega_j \geq 0, \quad \omega_1 = \omega_3, \quad \omega_2 = \omega_4, \quad \omega_5 = \omega_6 = \omega_7 = \omega_8, \quad \omega_0 = 1 - \sum_{j>0} \omega_j. \quad (\text{A1})$$

There are two lattice models that can be obtained as the subsets of the rD2Q9 lattice by setting some weight coefficients to be zero and removing some velocities in the rD2Q9 lattice. The first one is the rD2Q5I lattice, in which $\omega_j = 0$ ($j > 4$) and the discrete velocities \mathbf{c}_5 – \mathbf{c}_8 are removed. The second is the rD2Q5II lattice where $\omega_j = 0$ ($1 \leq j \leq 4$) and the discrete velocities \mathbf{c}_1 – \mathbf{c}_4 are removed.

For the rD3Q27 lattice,

$$\{\mathbf{c}_j, 0 \leq j \leq 6\} = \begin{pmatrix} 0 & c_1 & 0 & 0 & -c_1 & 0 & 0 \\ 0 & 0 & c_2 & 0 & 0 & -c_2 & 0 \\ 0 & 0 & 0 & c_3 & 0 & 0 & -c_3 \end{pmatrix}, \quad (\text{A2a})$$

$$\{\mathbf{c}_j, 7 \leq j \leq 18\} = \begin{pmatrix} c_1 & -c_1 & -c_1 & c_1 & c_1 & -c_1 & -c_1 & c_1 & 0 & 0 & 0 & 0 \\ c_2 & c_2 & -c_2 & -c_2 & 0 & 0 & 0 & 0 & c_2 & -c_2 & -c_2 & c_2 \\ 0 & 0 & 0 & 0 & c_3 & c_3 & -c_3 & -c_3 & c_3 & c_3 & -c_3 & -c_3 \end{pmatrix}, \quad (\text{A2b})$$

$$\{\mathbf{c}_j, 19 \leq j \leq 26\} = \begin{pmatrix} c_1 & c_1 & c_1 & -c_1 & -c_1 & -c_1 & -c_1 & c_1 \\ c_2 & c_2 & -c_2 & c_2 & -c_2 & -c_2 & c_2 & -c_2 \\ c_3 & -c_3 & c_3 & c_3 & -c_3 & c_3 & -c_3 & -c_3 \end{pmatrix},$$

$$\omega_j \geq 0, \quad \omega_1 = \omega_4, \quad \omega_2 = \omega_5, \quad \omega_3 = \omega_6, \quad \omega_7 = \omega_8 = \omega_9 = \omega_{10}, \quad \omega_{11} = \omega_{12} = \omega_{13} = \omega_{14},$$

$$\omega_{15} = \omega_{16} = \omega_{17} = \omega_{18}, \quad \omega_j = \omega_{19}(j > 19), \quad \omega_0 = 1 - \sum_{j>0} \omega_j. \quad (\text{A2c})$$

Similarly, we can obtain the following subsets of the rD3Q27 lattice:

- (i) For the rD3Q19 lattice, $\omega_{19} = 0$ and the discrete velocities \mathbf{c}_j ($j \geq 19$) are removed.
- (ii) For the rD3Q15 lattice, $\omega_7 = \omega_{11} = \omega_{15} = 0$ and the discrete velocities \mathbf{c}_j ($j = 7$ – 18) are removed.
- (iii) For the rD3Q13 lattice, $\omega_1 = \omega_2 = \omega_3 = \omega_{19} = 0$ and the discrete velocities \mathbf{c}_j ($j = 1$ – 6 , 19 – 26) are removed.
- (iv) For the rD3Q9 lattice, $\omega_j = 0$ ($1 \leq j \leq 18$) and the discrete velocities \mathbf{c}_j ($j = 1$ – 18) are removed.
- (v) For the rD3Q7 lattice, $\omega_j = 0$ ($j > 6$) and the discrete velocities \mathbf{c}_j ($j = 7$ – 26) are removed.

We note that the weight coefficient ω_j in the rDdQq lattice model can be determined by the velocity moment tensors. Let $\Delta^{(m)}$ be the m th-order moment of velocity set $\{\mathbf{c}_j, 0 \leq j \leq q-1\}$,

$$\Delta^{(m)} = \sum_j \omega_j \underbrace{\mathbf{c}_j \mathbf{c}_j \cdots \mathbf{c}_j}_m. \quad (\text{A3})$$

We can show that all of the odd-order moments are zero due to the lattice symmetry, and the even-order moments $\Delta^{(0)}$, $\Delta^{(2)}$, and $\Delta^{(4)}$ are used to determine the expression of the EDF f_j^{eq} . Actually, based on the weighted orthogonality between the zero- to second-order discrete Hermite polynomials \mathbf{c}_j^0 , \mathbf{c}_j and $\mathbf{Q}_j = \mathbf{c}_j \mathbf{c}_j - \Delta^{(2)}$, we have the following results for the quadratic EDF (44):

$$\sum_j \omega_j \mathbf{c}_j = 0, \quad \sum_j \omega_j \mathbf{Q}_j = 0, \quad \sum_j \omega_j \mathbf{c}_j \mathbf{Q}_j = 0, \quad (\text{A4})$$

$$\sum_j \omega_j \mathbf{c}_{j\alpha} \mathbf{c}_{j\beta} = 0, \quad \sum_j \omega_j \mathbf{Q}_{j\alpha\alpha} \mathbf{Q}_{j\beta\beta} = \Delta_{\alpha\alpha\beta\beta}^{(4)} - \Delta_{\alpha\alpha}^{(2)} \Delta_{\beta\beta}^{(2)} = 0, \quad \alpha \neq \beta. \quad (\text{A5})$$

Then we have

$$\Delta^{(0)} = \sum_j \omega_j = 1, \quad (\text{A6a})$$

$$\Delta^{(1)} = \sum_j \omega_j \mathbf{c}_j = 0, \quad \Delta^{(3)} = \sum_j \omega_j \mathbf{c}_j \mathbf{c}_j \mathbf{c}_j = 0, \quad (\text{A6b})$$

$$\Delta_{\alpha\beta}^{(2)} = \sum_j \omega_j \mathbf{c}_{j\alpha} \mathbf{c}_{j\beta} = 0, \quad \alpha \neq \beta, \quad (\text{A6c})$$

$$\Delta_{\alpha\alpha}^{(2)} = \sum_j \omega_j \mathbf{c}_{j\alpha}^2 = c_{s\alpha}^2 > 0, \quad (\text{A6d})$$

$$\Delta_{\alpha\alpha\beta\beta}^{(4)} = \sum_j \omega_j \mathbf{c}_{j\alpha}^2 \mathbf{c}_{j\beta}^2 = \Delta_{\alpha\alpha}^{(2)} \Delta_{\beta\beta}^{(2)} = c_{s\alpha}^2 c_{s\beta}^2, \quad \alpha \neq \beta, \quad (\text{A6e})$$

where the lattice speed $c_{s\alpha}$ is taken as a parameter along the α axis, as those in Refs. [17,19,36,37,60]. In the following, we present some details to determine the weight coefficients from Eqs. (A6a), (A6d), and (A6e).

For the rD2Q9 lattice [Eq. (A1)], it is easy to obtain the following results,

$$\Delta_{\alpha\alpha}^{(2)} = \sum_j \omega_j c_{j\alpha}^2 = 2c_\alpha^2(\omega_\alpha + 2\omega_5) = c_{s\alpha}^2, \quad (\text{A7})$$

$$\Delta_{\alpha\alpha\beta\beta}^{(4)} = 4c_\alpha^2 c_\beta^2 \omega_5 = c_{s\alpha}^2 c_{s\beta}^2, \quad \alpha \neq \beta, \quad (\text{A8})$$

and then one can derive

$$\omega_5 = \frac{c_{s1}^2 c_{s2}^2}{4c_1^2 c_2^2}, \quad \omega_\alpha = \frac{c_{s\alpha}^2}{2c_\alpha^2} - 2\omega_5 = \frac{c_{s\alpha}^2}{2c_\alpha^2} - \frac{c_{s1}^2 c_{s2}^2}{2c_1^2 c_2^2}, \quad \alpha = 1, 2, \quad \omega_0 = 1 - \sum_{j>0} \omega_j. \quad (\text{A9})$$

Letting $d_{0\alpha} = c_{s\alpha}^2/c_\alpha^2$, $\alpha = 1, 2$, we have

$$\omega_0 = (1 - d_{01})(1 - d_{02}), \quad \omega_1 = d_{01}(1 - d_{02})/2, \quad \omega_2 = (1 - d_{01})d_{02}/2, \quad \omega_5 = d_{01}d_{02}/4, \quad (\text{A10})$$

where $d_{01}, d_{02} \in (0, 1)$, or equivalently, $0 < c_{s1} < c_1$ and $0 < c_{s2} < c_2$.

Similarly, for the rD3Q27 lattice [Eq. (A2)], we have

$$\Delta_{11}^{(2)} = 2c_1^2(\omega_1 + 2(\omega_7 + \omega_{11}) + 4\omega_{19}) = c_{s1}^2, \quad (\text{A11a})$$

$$\Delta_{22}^{(2)} = 2c_2^2(\omega_2 + 2(\omega_7 + \omega_{15}) + 4\omega_{19}) = c_{s2}^2, \quad (\text{A11b})$$

$$\Delta_{33}^{(2)} = 2c_3^2(\omega_3 + 2(\omega_{11} + \omega_{15}) + 4\omega_{19}) = c_{s3}^2, \quad (\text{A11c})$$

$$\Delta_{1122}^{(4)} = 4c_1^2 c_2^2(\omega_7 + 2\omega_{19}) = c_{s1}^2 c_{s2}^2, \quad (\text{A12a})$$

$$\Delta_{1133}^{(4)} = 4c_1^2 c_3^2(\omega_{11} + 2\omega_{19}) = c_{s1}^2 c_{s3}^2, \quad (\text{A12b})$$

$$\Delta_{2233}^{(4)} = 4c_2^2 c_3^2(\omega_{15} + 2\omega_{19}) = c_{s2}^2 c_{s3}^2, \quad (\text{A12c})$$

which can be used to obtain

$$\omega_7 = \frac{c_{s1}^2 c_{s2}^2}{4c_1^2 c_2^2} - 2\omega_{19} = d_{01}d_{02}/4 - 2\omega_{19}, \quad (\text{A13a})$$

$$\omega_{11} = \frac{c_{s1}^2 c_{s3}^2}{4c_1^2 c_3^2} - 2\omega_{19} = d_{01}d_{03}/4 - 2\omega_{19}, \quad (\text{A13b})$$

$$\omega_{15} = \frac{c_{s2}^2 c_{s3}^2}{4c_2^2 c_3^2} - 2\omega_{19} = d_{02}d_{03}/4 - 2\omega_{19}, \quad (\text{A13c})$$

$$\omega_1 = \frac{c_{s1}^2}{2c_1^2} - 2(\omega_7 + \omega_{11}) - 4\omega_{19} = d_{01}(1 - d_{02} - d_{03})/2 + 4\omega_{19}, \quad (\text{A13d})$$

$$\omega_2 = \frac{c_{s2}^2}{2c_2^2} - 2(\omega_7 + \omega_{15}) - 4\omega_{19} = d_{02}(1 - d_{01} - d_{03})/2 + 4\omega_{19}, \quad (\text{A13e})$$

$$\omega_3 = \frac{c_{s3}^2}{2c_3^2} - 2(\omega_{11} + \omega_{15}) - 4\omega_{19} = d_{03}(1 - d_{01} - d_{02})/2 + 4\omega_{19}, \quad (\text{A13f})$$

$$\omega_0 = 1 - \sum_{j=1}^{26} \omega_j = 1 - (d_{01} + d_{02} + d_{03}) + d_{01}d_{02} + d_{01}d_{03} + d_{02}d_{03} - 8\omega_{19}, \quad (\text{A13g})$$

where $d_{0\alpha} = c_{s\alpha}^2/c_\alpha^2$ ($\alpha = 1, 2, 3$) and ω_{19} is a free weight coefficient.

From Eqs. (A13) and (A2), we can derive

$$\begin{aligned} 0 < 2\omega_1 + 4(\omega_7 + \omega_{11}) + 8\omega_{19} &= c_{s1}^2/c_1^2 = d_{01} < 1 \\ 0 < 2\omega_2 + 4(\omega_7 + \omega_{15}) + 8\omega_{19} &= c_{s2}^2/c_2^2 = d_{02} < 1 \\ 0 < 2\omega_3 + 4(\omega_{11} + \omega_{15}) + 8\omega_{19} &= c_{s3}^2/c_3^2 = d_{03} < 1. \end{aligned} \quad (\text{A14})$$

Then one can obtain $0 < \omega_{19} < d_{0\alpha}/8$ ($\alpha = 1, 2, 3$), while for some other lattice models, such as the rD3Q19 lattice, ω_{19} can be equal to zero.

Taking $\omega_{19} = d_{01}d_{02}d_{03}/8$ in Eq. (A13), we have

$$\omega_0 = (1 - d_{01})(1 - d_{02})(1 - d_{03}), \quad (\text{A15a})$$

$$\omega_1 = d_{01}(1 - d_{02})(1 - d_{03})/2, \quad \omega_2 = d_{02}(1 - d_{01})(1 - d_{03})/2, \quad \omega_3 = d_{03}(1 - d_{01})(1 - d_{02})/2, \quad (\text{A15b})$$

$$\omega_7 = d_{01}d_{02}(1 - d_{03})/4, \quad \omega_{11} = d_{01}d_{03}(1 - d_{02})/4, \quad \omega_{15} = d_{02}d_{03}(1 - d_{01})/4, \quad (\text{A15c})$$

where $d_{0\alpha} = c_{s\alpha}^2/c_\alpha^2 \in (0, 1)$ or $0 < c_{s\alpha} < c_\alpha$ ($\alpha = 1, 2, 3$).

From Eq. (A13), we can derive some special cases of the rD3Q27 lattice model:

(1) If we take $\omega_{19} = 0$, the weight coefficients in the rD3Q19 lattice model are obtained.

(2) If we take $\omega_7 = \omega_{11} = \omega_{15} = 0$, the weight coefficients in the rD3Q15 lattice model and the following relation can be obtained:

$$\frac{c_{s1}^2}{c_1^2} = \frac{c_{s2}^2}{c_2^2} = \frac{c_{s3}^2}{c_3^2}. \quad (\text{A16})$$

(3) If we take $\omega_1 = \omega_2 = \omega_3 = \omega_{19} = 0$, the weight coefficients in the rD3Q13 lattice model and the following condition can be derived:

$$\frac{c_{s1}^2}{c_1^2} = \frac{c_{s2}^2}{c_2^2} = \frac{c_{s3}^2}{c_3^2} = \frac{1}{2}. \quad (\text{A17})$$

It can be found from Eqs. (A16) and (A17) that when $c_{s1} = c_{s2} = c_{s3}$, one can get $c_1 = c_2 = c_3$, which implies that there are no rD3Q15 or rD3Q13 lattice models.

From Eqs. (A8), (A11), and (A12), we can give some constraints on the fourth-order moment $\Delta^{(4)}$ of discrete velocities for the rDdQq lattice model,

$$\Delta_{\alpha\alpha\alpha\alpha}^{(4)} = \sum_j \omega_j c_{j\alpha}^4 = c_\alpha^2 \Delta_{\alpha\alpha}^2 = c_\alpha^2 c_{s\alpha}^2, \quad \Delta_{\alpha\alpha\beta\beta}^{(4)} = \Delta_{\alpha\alpha}^{(2)} \Delta_{\beta\beta}^{(2)} = c_{s\alpha}^2 c_{s\beta}^2 \quad (\alpha \neq \beta), \quad \Delta_{\alpha\beta\gamma\theta}^{(4)} = 0 \quad (\text{else}), \quad (\text{A18})$$

which indicates that it no longer satisfies the isotropic condition on a rectangular lattice or on a standard lattice with $c_{s\alpha}^2 = c_s^2 \neq c^2/3$. Here we present its natural expression as the extension to that on the standard lattice:

$$\Delta^{(4)} = \langle \Delta^{(2)} \Delta^{(2)} \rangle + \delta^{(4)}, \quad (\text{A19})$$

where

$$\langle \Delta^{(2)} \Delta^{(2)} \rangle_{\alpha\beta\gamma\theta} = \Delta_{\alpha\beta}^{(2)} \Delta_{\gamma\theta}^{(2)} + \Delta_{\alpha\gamma}^{(2)} \Delta_{\beta\theta}^{(2)} + \Delta_{\beta\gamma}^{(2)} \Delta_{\alpha\theta}^{(2)}, \quad (\text{A20a})$$

$$\delta_{\alpha\beta\gamma\theta}^{(4)} = c_{s\alpha}^2 (c_\alpha^2 - 3c_{s\alpha}^2), \quad \alpha = \beta = \gamma = \theta, \quad \delta_{\alpha\beta\gamma\theta}^{(4)} = 0, \quad \text{else}. \quad (\text{A20b})$$

When the relations $c_{s\alpha} = c_s$ and $c_\alpha^2 = c^2 = 3c_s^2$ are satisfied for all α , one can obtain $\delta^{(4)} = 0$ and $\Delta^{(4)} = c_s^4 \Delta$ with $\Delta_{\alpha\beta\gamma\theta} = \delta_{\alpha\beta} \delta_{\gamma\theta} + \delta_{\alpha\gamma} \delta_{\beta\theta} + \delta_{\beta\gamma} \delta_{\alpha\theta}$, which means that the fourth-order isotropy can be achieved.

Remark 7. For the rD2Q5I, rD2Q5II, rD3Q7, and rD3Q9 lattice models, $\Delta_{\alpha\alpha\beta\beta}^{(4)} = c_{s\alpha}^2 c_{s\beta}^2$ ($\alpha \neq \beta$) does not hold. For the rD2Q5I lattice, $\omega_5 = 0$. Then we have $\omega_\alpha = \frac{c_\alpha^2}{2c_\alpha^2}$ ($\alpha = 1, 2$), while for the rD2Q5II lattice, $\omega_1 = \omega_2 = 0$, and we can obtain $\omega_5 = \frac{c_\alpha^2}{4c_\alpha^2}$ ($\alpha = 1, 2$) and also $\frac{c_{s1}^2}{c_1^2} = \frac{c_{s2}^2}{c_2^2}$. For the rD3Q9 lattice, $\omega_\alpha = 0$ ($1 \leq \alpha \leq 18$), we have $\omega_{19} = \frac{c_\alpha^2}{4c_\alpha^2}$ ($\alpha = 1, 2, 3$) and $\frac{c_{s1}^2}{c_1^2} = \frac{c_{s2}^2}{c_2^2} = \frac{c_{s3}^2}{c_3^2}$. For the rD3Q7 lattice, $\omega_\alpha = 0$ ($\alpha > 6$), we derive $\omega_\alpha = \frac{c_\alpha^2}{2c_\alpha^2}$ ($\alpha = 1, 2, 3$). Usually, the linear EDF $g_j^{eq}(\mathbf{A}, \mathbf{B}, \mathbf{0})$ is used, which satisfies Eq. (46) with $\mathbf{M} = 0$, while $\Delta^{(4)}$ does not satisfy Eqs. (A18) or (A19) since $\Delta_{\alpha\alpha\beta\beta}^{(4)} = c_{s\alpha}^2 c_{s\beta}^2$ ($\alpha \neq \beta$) does not necessarily hold.

Remark 8. From Eqs. (A10), (A13), and (A15) and Remark 7, we can find that there is no limitation to the aspect range of the present RMRT-LB method on a rDdQq lattice since only $d_{0\alpha} = c_{s\alpha}^2/c_\alpha^2$ or $c_s^2/c_\alpha^2 \in (0, 1)$ and the non-negativity of weight coefficients is required.

Remark 9. If we take $\omega_0 = 0$ or remove the rest velocity $\mathbf{c}_0 = \mathbf{0}$ in the rDdQq lattice model mentioned above, a rDdQ(q - 1) lattice model can be obtained.

APPENDIX B: DERIVATION OF THE NONLINEAR CONVECTION-DIFFUSION EQUATION FROM THE PRESENT RMRT-LB METHOD

The d -dimensional NCDE with a source term considered in this work can be expressed as [16,39]

$$\partial_t \phi + \nabla \cdot \mathbf{B} = \nabla \cdot [\mathbf{K} \cdot (\nabla \cdot \mathbf{D})] + S, \quad (\text{B1})$$

where ϕ is an unknown scalar function of position \mathbf{x} and time t , and S is a scalar source term. $\mathbf{B} = (\mathbf{B}_\alpha)$ is a vector function, $\mathbf{K} = (\mathbf{K}_{\alpha\beta})$ and $\mathbf{D} = (\mathbf{D}_{\alpha\beta})$ are symmetric positive definite matrices, and they can be functions of ϕ , \mathbf{x} , and t . It should be noted

that Eq. (B1) can be considered a general form of NCDE, and many different kinds of NCDEs considered in some previous work [35,38,42,69] are its special cases.

To recover Eq. (B1) from the RMRT-LB method [Eq. (1)], the unknown function ϕ can be calculated by $\phi = \sum_j f_j$ with the mass conservation $\sum_j f_j^{ne} = \sum_j (f_j - f_j^{eq}) = 0$, and the collision matrix \mathbf{A} and moments of f_j^{eq} , G_j , and F_j should satisfy the following relations [16]:

$$\sum_j \mathbf{e}_j \mathbf{A}_{jk} = s_0 \mathbf{e}_k, \quad \sum_j \mathbf{c}_j \mathbf{A}_{jk} = \mathbf{S}_{10} \mathbf{e}_k + \mathbf{S}_1 \mathbf{c}_k, \quad \forall k, \quad (\text{B2a})$$

$$\sum_j f_j^{eq} = \phi, \quad \sum_j \mathbf{c}_j f_j^{eq} = \mathbf{B}, \quad \sum_j \mathbf{c}_j \mathbf{c}_j f_j^{eq} = \beta c_s^2 \mathbf{D} + \mathbf{C}, \quad (\text{B2b})$$

$$\sum_j F_j = S, \quad \sum_j \mathbf{c}_j F_j = \mathbf{0}, \quad \sum_j G_j = 0, \quad \sum_j \mathbf{c}_j G_j = \mathbf{M}_{1G}, \quad (\text{B2c})$$

where \mathbf{S}_{10} is a $d \times 1$ matrix, \mathbf{S}_1 is an invertible $d \times d$ relaxation matrix corresponding to the diffusion matrix \mathbf{K} , β is a parameter for adjusting the relaxation matrix \mathbf{S}_1 in Eq. (B3), \mathbf{C} is an auxiliary moment, and \mathbf{M}_{1G} is the first-order moment of G_j .

We note that Eq. (B2) is the same as that of the standard MRT-LB model for NCDE (B1) in Ref. [16]. Here we omit the same process in recovering the macroscopic NCDE through the DTE analysis, and only give some useful results below, including the diffusion tensor \mathbf{K} , \mathbf{M}_{1G} , and the diffusion flux $-\mathbf{K} \cdot (\nabla \cdot \mathbf{D})$:

$$\mathbf{K} = \Delta t \beta c_s^2 (\mathbf{S}_1^{-1} - \mathbf{I}/2), \quad (\text{B3})$$

$$\mathbf{M}_{1G} = (\mathbf{I} - \mathbf{S}_1/2)(\partial_t \mathbf{B} + \nabla \cdot \mathbf{C}) = \begin{cases} (\mathbf{I} - \mathbf{S}_1/2) \mathbf{B}' S & \text{if } \mathbf{B} = \mathbf{B}(\phi) \text{ and } \mathbf{C} = \int \mathbf{B}' \mathbf{B}' d\phi \\ (\mathbf{I} - \mathbf{S}_1/2) \partial_t \mathbf{B} & \text{if } \mathbf{C} = \mathbf{0}, \end{cases} \quad (\text{B4})$$

$$-\mathbf{K} \cdot (\nabla \cdot \mathbf{D}) = \begin{cases} (\mathbf{I} - \mathbf{S}_1/2)(\mathbf{E} \mathbf{f}^{ne} + \Delta t \mathbf{B}' S/2) & \text{if } \mathbf{B} = \mathbf{B}(\phi) \text{ and } \mathbf{C} = \int \mathbf{B}' \mathbf{B}' d\phi \\ (\mathbf{I} - \mathbf{S}_1/2)(\mathbf{E} \mathbf{f}^{ne} + \Delta t \partial_t \mathbf{B}/2) & \text{if } \mathbf{C} = \mathbf{0}, \end{cases} \quad (\text{B5})$$

where $\mathbf{B}' = \frac{d\mathbf{B}}{d\phi}$, $\mathbf{f}^{ne} = (f_0^{ne}, f_1^{ne}, \dots, f_{q-1}^{ne})^T$. Additionally, if \mathbf{D} is only a function of ϕ , we can also obtain a local scheme for $\nabla \phi$ from Eq. (B5).

Actually, Eq. (B5) can be written as

$$\mathbf{E} \mathbf{f}^{ne} = \begin{cases} -(\mathbf{I} - \mathbf{S}_1/2)^{-1} (\mathbf{K} \cdot (\nabla \cdot \mathbf{D})) - \Delta t \mathbf{B}' S/2 & \text{if } \mathbf{B} = \mathbf{B}(\phi) \text{ and } \mathbf{C} = \int \mathbf{B}' \mathbf{B}' d\phi \\ -(\mathbf{I} - \mathbf{S}_1/2)^{-1} (\mathbf{K} \cdot (\nabla \cdot \mathbf{D})) - \Delta t \partial_t \mathbf{B}/2 & \text{if } \mathbf{C} = \mathbf{0}. \end{cases} \quad (\text{B6})$$

In addition, if we denote $\mathbf{m}_1^{ne} = \mathbf{E} \mathbf{f}^{ne}$, and consider Eq. (B6) and the mass conservation $\mathbf{e} \mathbf{f}^{ne} = \sum_j f_j^{ne} = 0$, one can obtain a useful formula to approximate f_j^{ne} ,

$$f_j^{ne} = g_j^{eq}(0, \mathbf{m}_1^{ne}, \mathbf{0}) = \omega_j \frac{\mathbf{c}_j \cdot \mathbf{m}_1^{ne}}{c_s^2} = \omega_j \frac{\mathbf{c}_{j\alpha} \mathbf{m}_{1,\alpha}^{ne}}{c_s^2}, \quad (\text{B7})$$

which can be used to initialize the distribution function f_j .

APPENDIX C: THE EQUILIBRIUM, AUXILIARY, AND SOURCE DISTRIBUTION FUNCTIONS OF THE RMRT-LB METHOD FOR THE NCDE

As discussed above, it can be found that to recover NCDE (B1) correctly, some proper requirements on the equilibrium, auxiliary, and source distribution functions should be satisfied. Based on Eqs. (44), (45), and (B2) for a rDdQq lattice model, we can obtain the following expressions of f_j^{eq} , G_j , and F_j with $c_{s\alpha} = c_s$ for all α :

$$\begin{aligned} f_j^{eq} &= g_j^{eq}(\phi, \mathbf{B}, \beta c_s^2 \mathbf{D} + \mathbf{C} - c_s^2 \phi \mathbf{I}) \\ &= \omega_j \left[\phi + \frac{\mathbf{c}_{j\alpha} \mathbf{B}_\alpha}{c_s^2} + \frac{(\beta c_s^2 \mathbf{D} + \mathbf{C} - c_s^2 \phi \mathbf{I})_{\alpha\alpha} (c_{j\alpha}^2 - c_s^2)}{c_s^2 (c_\alpha^2 - c_s^2)} + \frac{(\beta c_s^2 \mathbf{D} + \mathbf{C} - c_s^2 \phi \mathbf{I})_{\alpha\bar{\alpha}} (c_{j\alpha} c_{j\bar{\alpha}})}{2c_s^4} \right], \end{aligned} \quad (\text{C1})$$

$$G_j = g_j^{eq}(0, \mathbf{M}_{1G}, \mathbf{0}) = \omega_j \frac{\mathbf{c}_{j\alpha} \mathbf{M}_{1G,\alpha}}{c_s^2}, \quad F_j = g_j^{eq}(S, \mathbf{0}, \mathbf{0}) = \omega_j S, \quad (\text{C2})$$

where $\bar{\alpha}$ denotes the index γ with $\gamma \neq \alpha$, and \mathbf{M}_{1G} is given by Eq. (B4).

We note that if $\mathbf{D} = \phi \mathbf{I}$, NCDE (B1) would become

$$\partial_t \phi + \nabla \cdot \mathbf{B} = \nabla \cdot (\mathbf{K} \cdot \nabla \phi) + S. \quad (\text{C3})$$

If we further take $\beta = 1$ and $\mathbf{C} = \mathbf{0}$, f_j^{eq} , G_j , and F_j defined by Eqs. (C1) and (C2) can be simplified as

$$f_j^{eq} = g_j^{eq}(\phi, \mathbf{B}, \mathbf{0}) = \omega_j \left[\phi + \frac{\mathbf{c}_{j\alpha} \mathbf{B}_\alpha}{c_s^2} \right], \quad (\text{C4a})$$

$$G_j = g_j^{eq}(\mathbf{0}, (\mathbf{I} - \mathbf{S}_1/2) \partial_t \mathbf{B}, \mathbf{0}) = \omega_j \left[\frac{\mathbf{c}_{j\alpha} ((\mathbf{I} - \mathbf{S}_1/2) \partial_t \mathbf{B})_\alpha}{c_s^2} \right], \quad F_j = g_j^{eq}(S, \mathbf{0}, \mathbf{0}) = \omega_j S, \quad (\text{C4b})$$

where the term $\partial_t \mathbf{B}$ can be computed by the first-order explicit difference scheme, i.e., $\partial_t \mathbf{B} = [\mathbf{B}(\mathbf{x}, t) - \mathbf{B}(\mathbf{x}, t - \Delta t)] / \Delta t$. In this case, the simpler rDdQ2d or rDdQ(2d + 1) lattice model can be adopted.

In addition, we would also like to point out that at the diffusive scaling, the present RMRT-LB model can be further simplified [16]; i.e., the term $\frac{\Delta t^2}{2} \bar{D}_j F_j(\mathbf{x}, t)$ in the evolution equation [Eq. (1)] can be removed, and Eqs. (C1) and (C2) would reduce to

$$f_j^{eq} = g_j^{eq}(\phi, \mathbf{B}, \beta c_s^2 \mathbf{D} - c_s^2 \phi \mathbf{I}), \quad G_j = 0, \quad F_j = \omega_j S. \quad (\text{C5})$$

Remark 10. The first-order moment of f_j^{ne} , i.e., $\mathbf{E} f_j^{ne}$ in Eq. (B5), can also be computed by its counterpart ($\mathbf{E} f_j^{ne} = \mathbf{m}_E^{ne} - \mathbf{m}_E^{eq}$) in the moment space.

Remark 11. When \mathbf{K} and \mathbf{D} are diagonal matrices, the term $\beta c_s^2 \mathbf{D}$ in Eq. (B2b) can also be replaced by $\text{diag}(\beta_\alpha c_{s\alpha}^2 D_\alpha)$, and Eq. (B3) becomes

$$\kappa_\alpha = \Delta t (\tau - 1/2) \beta_\alpha c_{s\alpha}^2, \quad (\text{C6})$$

where $\mathbf{S}_1^{-1} = \tau \mathbf{I}$ has been used. In this case, the SRT-RLB model can be used for NCDE (B1), as shown in Ref. [35].

-
- [1] S. Chen and G. Doolen, Lattice Boltzmann method for fluid flows, *Annu. Rev. Fluid Mech.* **30**, 329 (1998).
- [2] S. Succi, *The Lattice Boltzmann Equation for Fluid Dynamics and Beyond* (Oxford University Press, Oxford, 2001); *The Lattice Boltzmann Equation for Complex States of Flowing Matter* (Oxford University Press, Oxford, 2018).
- [3] Z. Guo and C. Shu, *Lattice Boltzmann Method and Its Applications in Engineering* (World Scientific, Singapore, 2013).
- [4] T. Krüger, H. Kusumaatmaja, A. Kuzmin, O. Shardt, G. Silva, and E. M. Viggen, *The Lattice Boltzmann Method: Principles and Practice* (Springer, Switzerland, 2017).
- [5] D. d'Humières, Multiple-relaxation-time lattice Boltzmann models in three dimensions, *Philos. Trans. R. Soc. London A* **360**, 437 (2002).
- [6] M. Geier, M. Schönherr, A. Pasquali, and M. Krafczyk, The cumulant lattice Boltzmann equation in three dimensions: Theory and validation, *Comput. Math. Appl.* **70**, 507 (2015).
- [7] C. Pan, L.-S. Luo, and C. T. Miller, An evaluation of lattice Boltzmann schemes for porous medium flow simulation, *Comput. Fluids* **35**, 898 (2006).
- [8] L.-S. Luo, W. Liao, X. Chen, Y. Peng, and W. Zhang, Numerics of the lattice Boltzmann method: Effects of collision models on the lattice Boltzmann simulations, *Phys. Rev. E* **83**, 056710 (2011).
- [9] Z. Guo, K. Xu, and R. Wang, Discrete unified gas kinetic scheme for all Knudsen number flows: Low-speed isothermal case, *Phys. Rev. E* **88**, 033305 (2013).
- [10] Z. Guo and T. Zhao, Explicit finite-difference lattice Boltzmann method for curvilinear coordinates, *Phys. Rev. E* **67**, 066709 (2003).
- [11] X. He, L.-S. Luo, and M. Dembo, Some progress in lattice Boltzmann method. Part I. Nonuniform mesh grids, *J. Comput. Phys.* **129**, 357 (1996).
- [12] X. D. Niu, Y. T. Chew, and C. Shu, Simulation of flows around an impulsively started circular cylinder by Taylor series expansion- and least squares-based lattice Boltzmann method, *J. Comput. Phys.* **188**, 176 (2003).
- [13] O. Filippova and D. Hänel, Grid refinement for lattice-BGK models, *J. Comput. Phys.* **147**, 219 (1998).
- [14] Z. Guo, C. Zheng, and B. Shi, Domain-decomposition technique in lattice Boltzmann method, *Int. J. Mod. Phys. B* **17**, 129 (2003).
- [15] D. Lagrava, O. Malaspinas, J. Latt, and B. Chopard, Advances in multi-domain lattice Boltzmann grid refinement, *J. Comput. Phys.* **231**, 4808 (2012).
- [16] Z. Chai and B. Shi, Multiple-relaxation-time lattice Boltzmann method for the Navier-Stokes and nonlinear convection-diffusion equations: Modeling, analysis and elements, *Phys. Rev. E* **102**, 023306 (2020).
- [17] I. Ginzburg, Generic boundary conditions for lattice Boltzmann models and their application to advection and anisotropic-dispersion equations, *Adv. Water Resour.* **28**, 1196 (2005).
- [18] I. Ginzburg, Variably saturated flow described with the anisotropic lattice Boltzmann methods, *Comput. Fluids* **35**, 831 (2006).
- [19] I. Ginzburg and D. d'Humières, Lattice Boltzmann and analytical modeling of flow processes in anisotropic and heterogeneous stratified aquifers, *Adv. Water Resour.* **30**, 2202 (2007).
- [20] I. Ginzburg, Truncation errors, exact and heuristic stability analysis of two-relaxation-times lattice Boltzmann schemes for anisotropic advection-diffusion equation, *Commun. Comput. Phys.* **11**, 1439 (2012).

- [21] I. Ginzburg, Multiple anisotropic collisions for advection-diffusion lattice Boltzmann schemes, *Adv. Water Resour.* **51**, 381 (2013).
- [22] L. A. Hegele, Jr., K. Mattila, and P. Philippi, Rectangular lattice-Boltzmann schemes with BGK-collision operator, *J. Sci. Comput.* **56**, 230 (2013).
- [23] J. Koelman, A simple lattice Boltzmann scheme for Navier-Stokes fluid flow, *Europhys. Lett.* **15**, 603 (1991).
- [24] C. Peng, Z. L. Guo, and L.-P. Wang, A lattice-BGK model for the Navier-Stokes equations based on a rectangular grid, *Comput. Math. Appl.* **78**, 1076 (2019).
- [25] M. H. Saadat, B. Dorschner, and I. Karlin, Extended lattice Boltzmann model, *Entropy* **23**, 475 (2021).
- [26] Z. Wang and J. Zhang, Simulating anisotropic flows with isotropic lattice models via coordinate and velocity transformation, *Int. J. Mod. Phys. C* **30**, 1941001 (2019).
- [27] M. Bouzidi, D. d’Humières, P. Lallemand, and L.-S. Luo, Lattice Boltzmann equation on a two-dimensional rectangular grid, *J. Comput. Phys.* **172**, 704 (2001).
- [28] Y. Zong, C. Peng, Z. Guo, and L.-P. Wang, Designing correct fluid hydrodynamics on a rectangular grid using MRT lattice Boltzmann approach, *Comput. Math. Appl.* **72**, 288 (2016).
- [29] J. G. Zhou, MRT rectangular lattice Boltzmann method, *Int. J. Mod. Phys. C* **23**, 1250040 (2012).
- [30] C. Peng, H. Min, Z. Guo, and L.-P. Wang, A hydrodynamically-consistent MRT lattice Boltzmann model on a 2D rectangular grid, *J. Comput. Phys.* **326**, 893 (2016).
- [31] L.-P. Wang, H. D. Min, C. Peng, N. Geneva, and Z. Guo, A lattice-Boltzmann scheme of the Navier-Stokes equation on a three-dimensional cuboid lattice, *Comput. Math. Appl.* **78**, 1053 (2019).
- [32] E. Yahia and K. N. Premnath, Central moment lattice Boltzmann method on a rectangular lattice, *Phys. Fluids* **33**, 057110 (2021).
- [33] E. Yahia, W. Schupbach, and K. N. Premnath, Three-dimensional central moment lattice Boltzmann method on a cuboid lattice for anisotropic and inhomogeneous flows, *Fluids* **6**, 326 (2021).
- [34] V. Zecevic, M. Kirkpatrick, and S. Armfield, Rectangular lattice Boltzmann method using multiple relaxation time collision operator in two and three dimensions, *Comput. Fluids* **202**, 104492 (2020).
- [35] J. Lu, Z. Chai, B. Shi, Z. Guo, and G. Hou, Rectangular lattice Boltzmann model for nonlinear convection-diffusion equations, *Philos. Trans. R. Soc. A* **369**, 2311 (2011).
- [36] A. J. C. Ladd, Numerical simulations of particulate suspensions via a discretized Boltzmann equation. Part 1. Theoretical foundation, *J. Fluid Mech.* **271**, 285 (1994).
- [37] D. d’Humières, Generalized lattice-Boltzmann equations, in *Rarefied Gas Dynamics: Theory and Simulations*, Progress in Astronautics and Aeronautics Vol. 159 (AIAA, Washington, DC, 1992), pp. 450–458.
- [38] I. Ginzburg, Equilibrium-type and link-type lattice Boltzmann models for generic advection and anisotropic-dispersion equation, *Adv. Water Resour.* **28**, 1171 (2005).
- [39] Z. Chai, B. Shi, and Z. Guo, A multiple-relaxation-time lattice Boltzmann model for general nonlinear anisotropic convection-diffusion equations, *J. Sci. Comput.* **69**, 355 (2016).
- [40] Z. Chai and T. S. Zhao, Effect of the forcing term in the multiple-relaxation-time lattice Boltzmann equation on the shear stress or the strain rate tensor, *Phys. Rev. E* **86**, 016705 (2012).
- [41] H. Yoshida and M. Nagaoka, Multiple-relaxation-time lattice Boltzmann model for the convection and anisotropic diffusion equation, *J. Comput. Phys.* **229**, 7774 (2010).
- [42] B. Shi and Z. Guo, Lattice Boltzmann model for nonlinear convection-diffusion equations, *Phys. Rev. E* **79**, 016701 (2009).
- [43] X. He, S. Chen, and G. D. Doolen, A novel thermal model for the lattice Boltzmann method in incompressible limit, *J. Comput. Phys.* **146**, 282 (1998).
- [44] R. Du and B. Shi, A novel scheme for force term in the lattice BGK model, *Int. J. Mod. Phys. C* **17**, 945 (2006).
- [45] I. Ginzbourg and P. M. Adler, Boundary flow condition analysis for three-dimensional lattice Boltzmann model, *J. Phys. II France* **4**, 191 (1994).
- [46] A. Kuzmin, Z. Guo, and A. Mohamad, Simultaneous incorporation of mass and force terms in the multi-relaxation-time framework for lattice Boltzmann schemes, *Philos. Trans. R. Soc. A* **369**, 2219 (2011).
- [47] S. Chapman and T. G. Cowling, *The Mathematical Theory of Non-uniform Gases* (Cambridge University Press, Cambridge, UK, 1970).
- [48] U. Frisch, D. d’Humières, B. Hasslacher, P. Lallemand, Y. Pomeau, and J.-P. Rivet, Lattice gas hydrodynamics in two and three dimensions, *Complex Syst.* **1**, 649 (1987).
- [49] E. Ikenberry and C. Truesdell, On the pressures and the flux of energy in a gas according to Maxwell’s kinetic theory, I, *J. Ration. Mech. Anal.* **5**, 1 (1956).
- [50] W.-A. Yong, W. Zhao, and L.-S. Luo, Theory of the lattice Boltzmann method: Derivation of macroscopic equations via the Maxwell iteration, *Phys. Rev. E* **93**, 033310 (2016).
- [51] D. J. Holdych, D. R. Noble, J. G. Georgiadis, and R. O. Buckius, Truncation error analysis of lattice Boltzmann methods, *J. Comput. Phys.* **193**, 595 (2004).
- [52] A. Wagner, Thermodynamic consistency of liquid-gas lattice Boltzmann simulations, *Phys. Rev. E* **74**, 056703 (2006).
- [53] G. Kaehler and A. J. Wagner, Derivation of hydrodynamics for multi-relaxation time lattice Boltzmann using the moment approach, *Commun. Comput. Phys.* **13**, 614 (2013).
- [54] D. d’Humières and I. Ginzburg, Viscosity independent numerical errors for lattice Boltzmann models: From recurrence equations to “magic” collision numbers, *Comput. Math. Appl.* **58**, 823 (2009).
- [55] I. Ginzburg and L. Roux, Truncation effect on Taylor-Aris dispersion in lattice Boltzmann schemes: Accuracy towards stability, *J. Comput. Phys.* **299**, 974 (2015).
- [56] P. K. Kundu, I. M. Cohen, and D. Dowling, *Fluid Mechanics* (Academic Press, San Diego, CA, 2016).
- [57] P. J. Dellar, Bulk and shear viscosities in lattice Boltzmann equations, *Phys. Rev. E* **64**, 031203 (2001).
- [58] T. Krüger, F. Varnik, and D. Raabe, Second-order convergence of the deviatoric stress tensor in the standard Bhatnagar-Gross-Krook lattice Boltzmann method, *Phys. Rev. E* **82**, 025701(R) (2010).
- [59] W.-A. Yong and L.-S. Luo, Accuracy of the viscous stress in the lattice Boltzmann equation with simple boundary conditions, *Phys. Rev. E* **86**, 065701(R) (2012).

- [60] I. Ginzburg and D. d’Humières, Multi-reflection boundary conditions for lattice Boltzmann models, *Phys. Rev. E* **68**, 066614 (2003).
- [61] I. Ginzburg, F. Verhaeghe, and D. d’Humières, Two-relaxation-time lattice Boltzmann scheme: About parametrization, velocity, pressure and mixed boundary conditions, *Commun. Comput. Phys.* **3**, 427 (2008).
- [62] X. He and L.-S. Luo, Lattice Boltzmann model for the incompressible Navier-Stokes equation, *J. Stat. Phys.* **88**, 927 (1997).
- [63] M. Geier, A. Greiner, and J. G. Korvink, Cascaded digital lattice Boltzmann automata for high Reynolds number flow, *Phys. Rev. E* **73**, 066705 (2006).
- [64] C. Coreixas, B. Chopard, and J. Latt, Comprehensive comparison of collision models in the lattice Boltzmann framework: Theoretical investigations, *Phys. Rev. E* **100**, 033305 (2019).
- [65] L. Talon, D. Bauer, N. Gland, S. Youssef, H. Auradou, and I. Ginzburg, Assessment of the two relaxation time lattice Boltzmann scheme to simulate Stokes flow in porous media, *Water Resour. Res.* **48**, W04526 (2012).
- [66] S. Khirevich, I. Ginzburg, and U. Tallarek, Coarse- and fine-grid numerical behavior of MRT/TRT lattice-Boltzmann schemes in regular and random sphere packings, *J. Comput. Phys.* **281**, 708 (2015).
- [67] Z.-L. Guo, C.-G. Zheng, and B.-C. Shi, Non-equilibrium extrapolation method for velocity and pressure boundary conditions in the lattice Boltzmann method, *Chin. Phys.* **11**, 366 (2002).
- [68] U. Ghia, K. N. Ghia, and C. Shin, High-Re solutions for incompressible flow using the Navier-Stokes equations and a multigrid method, *J. Comput. Phys.* **48**, 387 (1982).
- [69] Z. Chai, H. Liang, R. Du, and B. Shi, A lattice Boltzmann model for two-phase flow in porous media, *SIAM J. Sci. Comput.* **41**, B746 (2019).